Quaternary Science Reviews 287 (2022) 107549

Contents lists available at ScienceDirect

Quaternary Science Reviews

journal homepage: www.elsevier.com/locate/quascirev

The last deglaciation of Alaska and a new benchmark ^{10}Be moraine chronology from the western Alaska Range

Joseph P. Tulenko [a, c, *], Jason P. Briner [a], Nicolás E. Young [b], Joerg M. Schaefer [b]

[a] University at Buffalo, Buffalo, NY, 14260, USA
[b] Lamont-Doherty Earth Observatory, Palisades, NY, 10694, USA
[c] Berkeley Geochronology Center, Berkeley, CA, 94709, USA

ARTICLE INFO

Article history:
Received 7 February 2022
Received in revised form
20 April 2022
Accepted 29 April 2022
Available online xxx

Handling Editor: Dr C. O'Cofaigh

ABSTRACT

We report 50 new and 22 previously published ^{10}Be ages from 15 distinct moraine crests in the western Alaska Range spanning from the Last Glacial Maximum (LGM) terminal moraine to a latest Pleistocene moraine immediately down valley from late Holocene moraines. Moraines were deposited between 21.3 ± 0.8 ka and 12.8 ± 0.6 ka and conform morphostratigraphically, giving us high confidence in the chronology. Our record, and the key records reviewed in our compilation from across Alaska indicate a culmination of the regional LGM between ca. 21–19 ka. Our chronology, unmatched in resolution from a single valley in Alaska, indicates that steady glacier recession from ca. 21–18 ka was punctuated by accelerated retreat from ca. 17–16 ka, followed by a period of prolonged moraine deposition between ca. 16 and 15 ka. After ca. 15 ka rapid glacier retreat was punctuated by a re-advance ca. 12.8 ka. Other chronologies across Alaska show further evidence of moraine deposition between ca. 16–15 ka and ca. 13–12 ka. The emerging pattern of glacier retreat through the last deglaciation in Alaska is compared to several global, regional, and local climate proxies to assess what climate factors controlled the timing and pace of glacier retreat in Alaska. We hypothesize that warming caused by rising boreal summer insolation drove initial and steady deglaciation from the LGM terminal moraine position until ca. 18 ka, after which time global warming from rising CO_2 concentrations accelerated retreat. Subsequent periods of moraine deposition in Alaska coincide with decreasing trends in the NGRIP ice core record, at the culmination of Heinrich Stadial 1 (ca. 16–15 ka), and during the early Younger Dryas between 13 and 12.5 ka. While comparisons are made between alpine glacier records and the timing of other geologic events that may have impacted local-to-regional climate (e.g., the opening of the Bering Strait, the saddle collapse between the Laurentide and Cordilleran Ice sheets, and post-LGM Bering Sea dynamics), the relationship between our record and these geologic events are ambiguous. We suggest glaciers across Alaska were possibly more sensitive to other regional and global climate forcing mechanisms, mainly rising insolation, global CO_2 rise, and Northern Hemisphere Ocean circulation forcing through deglaciation.

1. Introduction

The behavior of alpine glaciers is tightly coupled to climate (Oerlemans, 2005) and archives of their past advance and retreat provide proxy records of past climate change (Shakun et al., 2015; Roe et al., 2017). The last deglaciation (ca. 19 to 11.6 ka; Clark et al., 2012) was a crucial time of transition from global ice age to interglacial conditions. Embedded within net global warming and glacier retreat were several spatially heterogeneous, rapid climate events that influenced timelines of glacier change (Rasmussen et al., 2014; Pedro et al., 2016). Detailed moraine sequences have been meticulously mapped and dated in multiple locations across the globe (e.g., Putnam et al., 2013; Shakun et al., 2015; Laabs et al., 2020; Peltier et al., 2021; Palacios et al., 2020), and reveal varied responses to the complex and spatially heterogeneous pattern of climate change through the last deglaciation. For example, multiple valleys in the southern Alps of New Zealand and in the southern Andes mountains reveal a pattern of retreat that mirrors the atmospheric CO_2 pattern recorded in Antarctic ice cores (e.g., Putnam

* Corresponding author. University at Buffalo, Buffalo, NY, 14260, USA.
E-mail address: jptulenk@buffalo.edu (J.P. Tulenko).

https://doi.org/10.1016/j.quascirev.2022.107549
0277-3791/

et al., 2010; Putnam et al., 2013; Moreno et al., 2015; Hall et al., 2017; Barrell et al., 2019). In comparison, moraine ages from the western United States reveal that glaciers remained at or near their LGM terminal moraines until ca. 17–16 ka, after the initial rise in CO_2 (Young et al., 2011; Laabs et al., 2020; Tulenko et al., 2020a). Whereas detailed retreat histories of alpine glaciers through the last deglaciation have arisen from multiple locations across the globe, there is a notable lack of detailed alpine glacier chronologies in the high northern latitudes spanning the last deglaciation.

Throughout the Pleistocene, as continental ice sheets fluctuated over multiple glacial cycles across much of the high northern latitudes, Beringia remained comparatively ice-free (Duk-Rodkin, 1999; Kaufman et al., 2011; Sheinkman, 2011). Instead, glacier advances in Beringia were restricted to high mountain centers. In Alaska, mountain glaciers flowed out from the Brooks Range, the northern and western sections of the Alaska Range, the Ahklun Mountains and other various smaller ranges across interior Alaska (Porter et al., 1983; Hamilton et al., 1986; Kaufman et al., 2011, Fig. 1). Southern (coastal) Alaska was glaciated by large, converged ice masses that formed the western extension of the Cordilleran Ice Sheet, and in some places, ice extended well offshore (Mann and Peteet, 1994; Reger et al., 2007; Lesnek et al., 2018, 2020; Haeussler et al., 2021). While there is a rich history spanning over five decades of glacial mapping efforts in Alaska (Coulter et al., 1965; Porter et al., 1983; Hamilton et al., 1986; Kaufman et al., 2011), moraines deposited in mountain ranges across the state have not yet been dated in as much detail as sites at lower latitudes. Indeed, a great deal is known about the timing of LGM culmination across the state (e.g., Briner et al., 2017), yet there is less known about the timing and rate of post-LGM alpine deglaciation. Determining the timing and rate of alpine deglaciation may give insight into which climatic mechanisms, such as high northern latitude insolation forcing (Laskar et al., 2004; Pendleton et al., 2015), global CO_2 forcing (Shakun et al., 2012, 2015), Northern Hemisphere ocean circulation (Wang et al., 2001; NGRIP members, 2004; Praetorius et al., 2020), Bering Land Bridge dynamics (Elias et al., 1996; Brigham-Grette, 2001; Daniels et al., 2021), and North American ice sheet influence on atmospheric circulation (Lora et al., 2016; Löfverström and Liakka, 2016; Tulenko et al., 2020b) were most important for driving glacier changes.

Here, we review the available chronologies of alpine glacier retreat in Alaska that span the last deglaciation. The chronologies

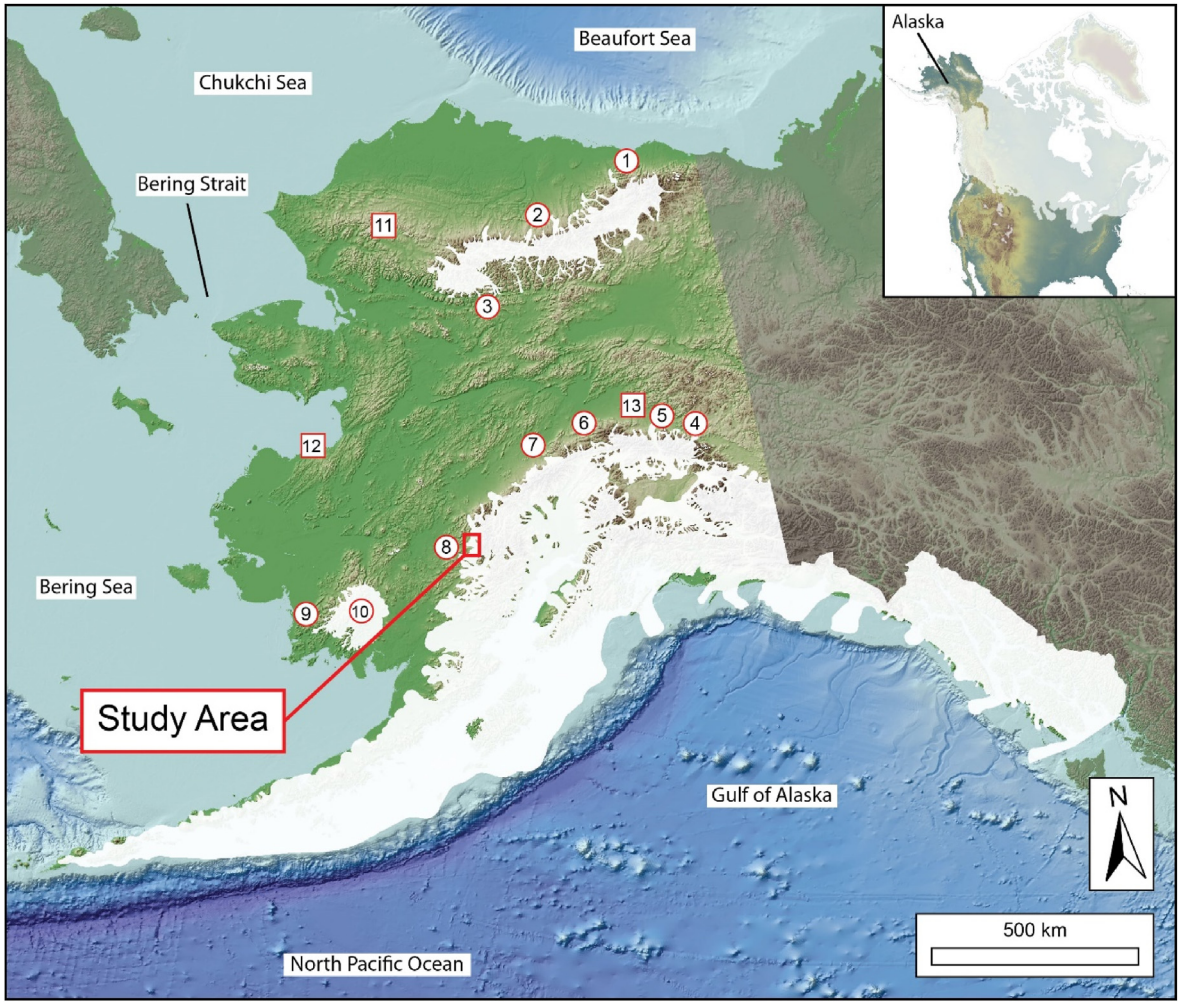

Fig. 1. Last Glacial Maximum ice extent in Alaska (ice limits from the Alaska PaleoGlacier Atlas; http://akatlas.geology.buffalo.edu/; Kaufman et al., 2011). Numbered red circles are sites with alpine glacier chronologies, numbered red squares are sites with other paleo-environmental reconstructions. 1) northeastern Brooks Range, 2) central Brooks Range, 3) south-central Brooks Range, 4) Fish Lake valley, eastern Alaska Range 5) Delta River valley, eastern Alaska Range, 6) Nenana River valley, central Alaska Range, 7) Denali National Park (including Wonder Lake), 8) The Farewell Region, 9) southwestern Ahklun Mountains, 10) Waskey Mountain site, 11) Burial Lake, 12) Zagoskin Lake, 13) Harding and Birch Lakes. Note that abundant valley glaciers existed in the small ranges across interior Alaska and on the Seward Peninsula but are not shown at this scale. (For interpretation of the references to color in this figure legend, the reader is referred to the Web version of this article.)

are then placed, along with our new, detailed chronology of alpine glacier retreat from the Revelation Mountains in the western Alaska Range, in the context of regional and global climate changes mentioned previously. The new chronology from the Revelation Mountains is based on 50 new cosmogenic ^{10}Be exposure ages (hereafter referred to as ^{10}Be ages) from boulders embedded in 11 distinct moraines deposited in the North Swift River valley. The new chronology is then combined with a previously published chronology from a neighboring valley (Tulenko et al., 2018) to generate a near-continuous master record of alpine glacier retreat from the culmination of the LGM through the entire deglacial period for the Revelation Mountains. We then review what possible climatic forcing mechanisms were the dominant control on deglaciation across Alaska.

2. A review of climate and glacier change in Alaska during the last deglaciation

2.1. Climate change in Alaska during the last deglaciation

The presence of large ice-free areas in Alaska during the Pleistocene allows for opportunities to reconstruct past climate in the region via paleoenvironmental proxies (primarily summer temperature proxies) stored in natural archives, predominantly continuous lake sediment records. A synthesis of pollen assemblages across Alaska from several lakes (n = 47) indicates that the summer temperature depression in Alaska during the LGM was around 4 °C relative to June-July-August monthly mean values from 1960 to 1990 (Whitmore et al., 2005; Viau et al., 2008, Fig. 2). Furthermore, summer temperatures inferred from fossil chironomids at Zagoskin Lake (Yukon Delta; Fig. 1 location 12) and at Burial Lake (northwest Brooks Range; Fig. 1 location 11) also reveal summer temperature depressions around 4 °C, in support of the pollen data (Kurek et al., 2009). The Zagoskin Lake record shows steady, modest warming beginning ca. 22 ka, with a brief interruption between ca. 16–15 ka, and then a continuation of warming to the onset of the Holocene. The Burial Lake record indicates that cooler summer temperatures may have persisted until ca. 17 ka, after which there was steady warming that leveled off near the onset of the Holocene. A recent reconstruction of summer temperature inferred from leaf wax hydrogen isotope data measured in a sediment core from the North Slope of the Brooks Range (Fig. 1; location 2) reveals a similar pattern of approximate 4 °C LGM cooling and delayed warming beginning ca. 17 ka (Daniels et al., 2021). Embedded within the overall pattern of warming within the record from Daniels et al. (2021) are periods of cooling that appear to correlate with climatic events observed in the North Atlantic, such as the Older and Younger Dryas periods.

Proxy evidence from lake-level reconstructions (Burial Lake, Fig. 1, location 11; Abbott et al., 2010; Finkenbinder et al., 2015); Harding Lake (Fig. 1, location 13; Finkenbinder et al., 2014), and S-Ratios measured in lake sediments – a ratio of the low and high coercivity magnetic materials used as a proxy of dust flux (Burial Lake; Fig. 1 location 11; Dorfman et al., 2015) – indicate that Alaska was likely much drier during the LGM and experienced increasing precipitation through the last deglaciation. Pollen assemblage data collected across the state also suggest that total annual precipitation was lower (ca. 125 mm less at most) than modern values (long-term monthly mean from 1960 to 1990; Whitmore et al., 2005) during the LGM and through much of the deglaciation (Viau et al., 2008). There is a notable increase in total annual precipitation (ca. 250 mm) during the Younger Dryas interval observed from pollen data statewide, which appears to correlate with increasing winter temperatures (Viau et al., 2008; Kaufman et al., 2010). Kaufman et al. (2010) suggest the correlation may indicate a strengthening

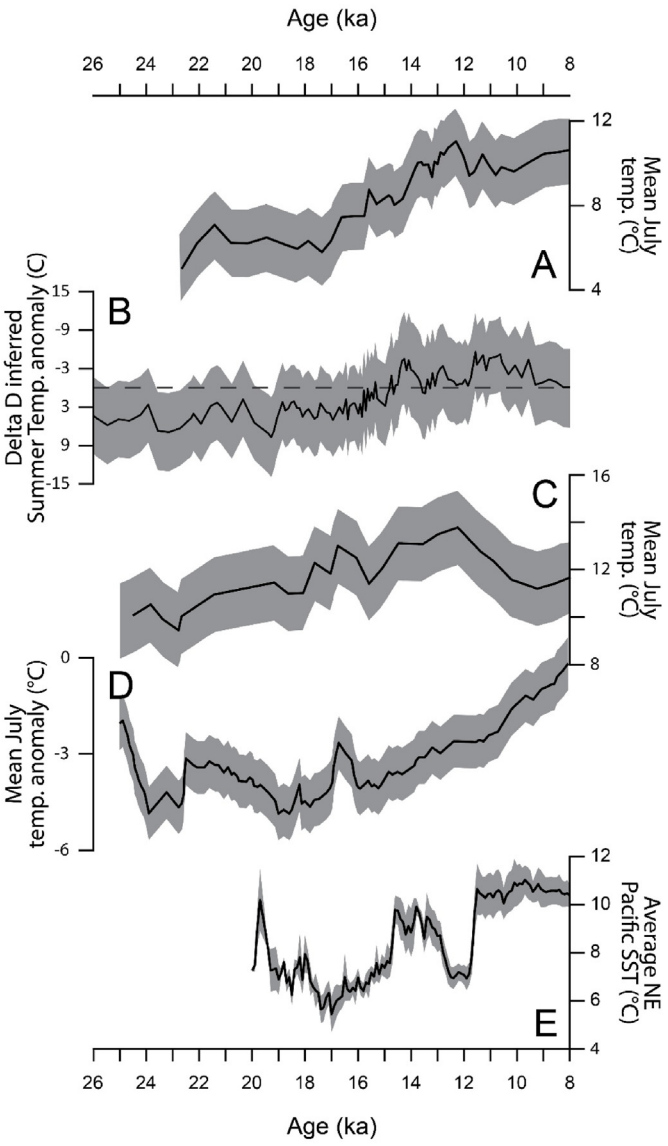

Fig. 2. Paleoclimate proxy records from across Alaska that span the full deglaciation arranged from north to south. A) Fossil chironomid-based summer temperature reconstruction from Burial Lake (Fig. 1, location 11; Kurek et al., 2009). B) Delta deuterium-inferred summer temperature reconstruction from the north-central Brooks Range (Fig. 1, location 2; Daniels et al., 2021). C) Fossil chironomid-based summer temperature reconstruction from Zagoskin Lake (Fig. 1 location 12; Kurek et al., 2009). D) Pollen-based summer temperature reconstruction from the top five analogues analyzed across Alaska (Viau et al., 2008). E) Average northeast Pacific Ocean mean annual sea surface temperatures (Praetorius et al., 2020). Broadly, proxy data reveal a ca. 4 °C temperature depression in Alaska during the LGM, but heterogeneity in the timing of warming through the last deglaciation.

of the Aleutian Low - a predominantly wintertime phenomena - through the Younger Dryas interval, which could have led to enhanced glacier growth during the Younger Dryas.

In summary, available paleoclimate records from Alaska indicate a summer temperature depression during the LGM of approximately 4 °C (Fig. 2), which is mild relative to other parts of the Arctic (Tierney et al., 2020; Osman et al., 2021) and the mid-to-low latitudes (Seltzer et al., 2021). This magnitude of temperature depression in Alaska generally agrees with model simulations (e.g., Löfverström and Liakka, 2016) and recent data-assimilation results (Tierney et al., 2020). A limited temperature depression and relatively drier conditions in Alaska during the LGM is consistent with

Table 1
Correlation of key glacial deposits in Alaska referenced in this study. For more detailed descriptions and correlations for regions beyond the ones reviewed in this study, readers are referred to Hamilton (1994).

Global	Marine Isotope Stage	North America	Brooks Range	Denali NP	NW Alaska Range	Revelation Mountains
Deglaciation (19–11.7 ka)	**MIS 2** (29–11.7 ka; Lisiecki and Raymo, 2005)	**Late Wisconsin** (Porter et al., 1983)	**Itkillik-2** (Hamilton et al., 1986)	MP-IVMP-IIIMP-IIMP-I**McKinley Park MP-I - MP-IV** (Ten Brink and Waythomas, 1985)	F2-IVF2-IIIF2-IIF2–I**Farewell-2 F2-I - F2-IV** (Kline and Bundtzen, 1986)	F2-IVF2-IIIF2-IIF2–I **Farewell-2 F2-I - F2-IV** ()
LGM (26–19 ka)						
Pre-LGM (>26 ka)	**MIS 4** (71–57 ka; Lisiecki and Raymo, 2005)	**Early Wisconsin** (Porter et al., 1983)	**Itkillik-1** (Hamilton et al., 1986)	- - -	**Farewell-1** (Kline and Bundtzen, 1986)	**Farewell-1** (Tulenko et al., 2018)

extent of glaciation across the state in that glaciers were restricted to mountain ranges, leaving much of Alaska ice-free. Proxy reconstructions, however, reveal some spatial heterogeneity in the timing of warming following the LGM, where data from near the Brooks Range shows a delay in warming compared to other locations. Daniels et al. (2021) argue that some discrepancies in Brooks Range warming compared to the rest of the state may be due to seasonality and how different proxies are sensitive to different seasonal feedbacks (i.e., wintertime sea ice expansion increasing local albedo, among other feedbacks), but generally these discrepancies remain unresolved.

Numerous marine sediment records from the Northeast Pacific Ocean and Bering Sea also shed light on climate variability in the region through the deglacial period. Praetorius et al. (2020) summarizes available ocean sediment records from the Northeast Pacific region (n = 12; see citations within) to show a sea surface temperature (SST) depression around 4 °C (relative to 20th century estimates) from ca. 20 to ca. 15 ka, culminating at ca. 17 ka (Fig. 2). This period of cooling is followed by warming, up until a roughly 3° decrease in temperature during the subsequent Younger Dryas. The cooling and warming pattern through Heinrich Stadial 1 may have influenced the advance and culmination of the ocean-terminating Cordilleran Ice Sheet (CIS) margin from ca. 19 to ca. 17 ka (Lesnek et al., 2018), and subsequent retreat between ca. 17–15 ka (Lesnek et al., 2020). The chronology from terrestrial records of CIS margin fluctuations is supported by significant increases in ice-rafted debris (IRD) between ca. 17–16 ka observed in a sediment core offshore Vancouver Island, potentially indicating significant ice sheet retreat through that interval (Cosma and Hendy, 2008). Caissie et al. (2010) use diatom assemblages to suggest that the Bering Sea became more frequently ice free through the last deglaciation, with major shifts from perennial sea ice cover to seasonal ice cover at ~15 ka, and then virtually ice-free conditions by ~11 ka. Furthermore, planktic oxygen isotope measurements in the same study indicate progressively increasing sea surface temperatures in the Bering Sea through the last deglaciation. The Bering Sea provides a moisture source for interior Alaska, so changes in moisture availability may have an impact on alpine glaciers there.

2.2. Glacier fluctuations in Alaska during the last deglaciation

While there are rich sequences of glacial deposits in southern and southeast Alaska that have been thoroughly mapped and, in some cases, dated (e.g., Mann and Peteet, 1994; Reger et al., 2007; Kopczynski et al., 2017; Lesnek et al., 2018, 2020; Haeussler et al., 2021), our review largely excludes records from the relatively complicated and merged ice masses in southern Alaska that may have behaved differently from independent alpine glaciers across the rest of the state. Here, we review pre-existing chronologies of alpine glaciation in Alaska that span the last deglaciation (ca. 19–11.6 ka; Table 1).

Glacial deposits from the LGM and subsequent deglaciation are thoroughly mapped in the Brooks Range (locally termed the Itkillik Glaciation; Hamilton, 1986) and moraines in a few alpine valleys in the region have been dated. Two separate sites, one in the central Brooks Range (Fig. 1, location 2), and the other in the northeastern Brooks Range (Fig. 1, location 1) appear to show different LGM culminations at 21.0 ± 0.8 ka (n = 5, excluding 4 outliers; Pendleton et al., 2015) and 25.6 ± 3.1 ka (n = 4, excluding one outlier; Balascio et al., 2005), respectively. Whether the relatively high scatter and mismatch in culmination ages is caused by issues with isotopic inheritance and/or post-depositional disruption, or if the differences truly reflect two separate advance culminations remains unknown. Regardless, ^{10}Be ages

generally conform with radiocarbon constraints on down valley LGM outwash sequences that suggest glaciers were expanded in the Brooks Range between ca. 27–23 cal ka (Hamilton et al., 1986). In the northeastern Brooks Range (Fig. 1, location 1), a second moraine up-valley of the mapped LGM moraine is dated to 20.7 ± 2.8 ka (n = 4; Balascio et al., 2005), so it is possible that this moraine corresponds to the LGM moraine dated in the central Brooks Range. Mapping efforts across the Brooks Range indicate that post-LGM moraines in most valleys only exist just beyond and/or within valley cirques; moraines further down-valley between cirques and LGM limits were either not preserved following deglaciation or were simply not deposited. Some cirque and near-cirque moraines in the Brooks Range have been dated. One site in the north-central Brooks Range (Fig. 1, location 2) contains a moraine positioned ca. 4 km down-valley from the cirque (approximately 5% the distance of an undated mapped LGM moraine) that dates to 17.2 ± 1.0 ka (n = 4; Pendleton et al., 2015). In four separate valleys across the central Brooks Range (Fig. 1, locations 2 and 3), several erratics (i.e., glacially transported boulders sourced from up-valley bedrock and not associated with moraine landforms) and moraine boulders deposited directly outboard of each respective valley cirque range in age between ca. 16–14 ka, indicating that any subsequent advances (e.g., possible advances in response to Younger Dryas cooling) were limited to within late Holocene cirque glacier extents (Badding et al., 2013; Pendleton et al., 2015).

Glaciation across the Alaska Range during the LGM was widespread and is well-mapped (Porter et al., 1983; Ten Brink and Waythomas, 1985; Hamilton et al., 1986; Kaufman and Manley, 2004; Kaufman et al., 2011). Alpine glacier moraines in multiple locations along the northern and western limbs of the range have also been surveyed and dated. From east to west, terminal moraines dated in the Fish Lake River valley (Fig. 1 location 4), the Donnelly Dome region (Fig. 1 location 5), and the Wonder Lake region in Denali National Park (Fig. 1 location 7) indicate an LGM culmination of 18.7 ± 0.2 ka (n = 4, excluding 3 outliers; Young et al., 2009), 19.4 ± 0.9 ka (n = 6, excluding 5 outliers; Matmon et al., 2010), and between 21.5 and 20.7 ka (based on radiocarbon dates of organic material incorporated in deposits above and below the terminal moraine; Ten Brink and Waythomas, 1985). There are a few other sites with existing chronologies, but terminal moraine ages are difficult to interpret (e.g., Nenana River valley; Dortch et al., 2010a, Fig. 1 location 6).

In a few of the aforementioned sites, moraines and erratic boulders deposited between LGM terminal moraines and valley cirques have been dated. In the Fish Lake valley, erratic boulders emplaced just beyond late Holocene moraines and extant glaciers cluster in two groups at 15.9 ± 1.1 ka (n = 3) and 12.9 ± 0.2 ka (n = 3), respectively (excluding 4 outliers; Young et al., 2009). In the Delta River valley, the terminal LGM moraine is dated to 19.4 ± 0.9 (n = 6, excluding 5 outliers; Matmon et al., 2010). A recessional moraine in the Delta River valley dates to 15.2 ± 0.7 ka (n = 4; Howley, 2008; Briner et al., 2017). Farther west, in the Nenana River valley, a moraine within the LGM limit is dated at 17.9 ± 1.6 ka (n = 7, excluding 1 outlier; Dortch et al., 2010a). Erratic boulders from two separate locations in the region date to 17.4 ± 2.2 ka and 15.2 ± 0.5 ka (Dortch et al., 2010a). These two locations are in separate valleys from the LGM moraine dated in the nearby Nenana River valley, and so it is difficult to place all three sites within stratigraphic context of each other.

Denali National Park hosts perhaps the most robust deglaciation chronology in the Alaska Range (Fig. 1, location 7). The McKinley Park four-fold moraine sequence has radiocarbon constraints from above and below the MP-I till units (terminal LGM position), from stratigraphic sequences observed in sediment cores recovered from Wonder Lake situated stratigraphically between the MP-II and MP-III units, and from stratigraphic units above and below the MP-IV end moraine. Radiocarbon ages have been interpreted to suggest the MP-I, MP-II, MP-III, and MP-IV moraines were deposited at 21.5–20.7 ka, 20.7–17.1 ka, 15.1–14.6 ka, and 12.1–11.5 ka, respectively (Ten Brink and Waythomas, 1985; Werner et al., 1993; Child, 1995). There have been attempts to corroborate the radiocarbon chronology with ^{10}Be dating, but results are largely inconclusive (Dortch et al., 2010b). ^{10}Be ages are difficult to interpret, likely because these moraines are draped over the active Denali Fault and/or because of the surging nature of the Muldrow Glacier (Harrison, 1964). Faulting and seismic activity could enhance moraine degradation, and moraines formed from surging are potentially less stable than those that are built over longer periods at more stable glacier margins. Both factors would likely lead to enhanced boulder instability, which could produce many younger-than-expected ^{10}Be ages.

The Ahklun Mountains in southwestern Alaska hosted an independent ice cap multiple times throughout the Pleistocene, including the LGM (Kaufman et al., 2011, Fig. 1, locations 9 and 10). Deposits from major outlet glaciers draining radially outward from the ice-cap center have been well-mapped and, in a few locations, well-dated (Manley et al., 2001; Kaufman et al., 2011). Within a sediment core collected from a formerly ice-dammed lake in the southwest Ahklun Mountains (Fig. 1 location 9), bracketing radiocarbon ages constrain a minerogenic unit associated with the advance of an outlet glacier during the LGM to between 23.9 and 19.4 cal ka (Kaufman et al., 2003, 2012). Two recessional moraines slightly up-valley of the LGM terminal moraine are associated with a radiocarbon age of ca. 20.4 cal ka that is a minimum age for the first recessional moraine and maximum age for the second recessional moraine (Manley et al., 2001). The only location in the Ahklun Mountains with chronologic constraints on younger moraines is from near Waskey Mountain (Fig. 1 location 10). Young et al. (2019) updated the chronology from a set of late-glacial moraines generated in Briner et al. (2002) with new ^{10}Be ages from boulders deposited on an outermost moraine that dates 12.5 ± 0.2 ka (n = 7); an inner moraine to 12.1 ± 0.5 ka (n = 6). These ages also conform with radiocarbon constraints from a lake impounded by the moraines with a basal minimum-limiting age of ca. 11 cal ka (Levy et al., 2004). The Waskey Moraines are located at approximately 5% of the down-valley distance between the cirque and the terminal LGM position. While the exact timing and pace of deglaciation is unknown, at some point between ca. 20 ka and ca. 12.5 ka, there must have been substantial retreat, which could have been either gradual or protracted.

While there remain relatively few chronologic constraints on the timing and pace of alpine glacier retreat in Alaska through the last deglaciation, the key chronologies summarized here display a few emerging patterns. Primarily, it appears that Alaska-wide LGM glacier advances culminated roughly in-step with the closing of the global LGM between ca. 21–19 ka. Following this, it appears that many glaciers were in steady retreat, with sufficient pausing or readvancing in some locations to have generated moraines, until the latter stages of Heinrich Stadial 1 (ca. 18–15 ka). Of the chronologies reviewed here, it is apparent that several recessional moraines date to 16–15 ka, at approximately 40–30% of LGM extents, indicating that there may have been widespread glacier stability or re-advance around this time. This is not the case for all glaciers in Alaska, however, as is shown in the Brooks Range where all existing evidence thus far suggests glaciers had retreated to within their cirques by ca. 15 ka. Finally, there are also a few chronologies that indicate glacier advances during the Younger

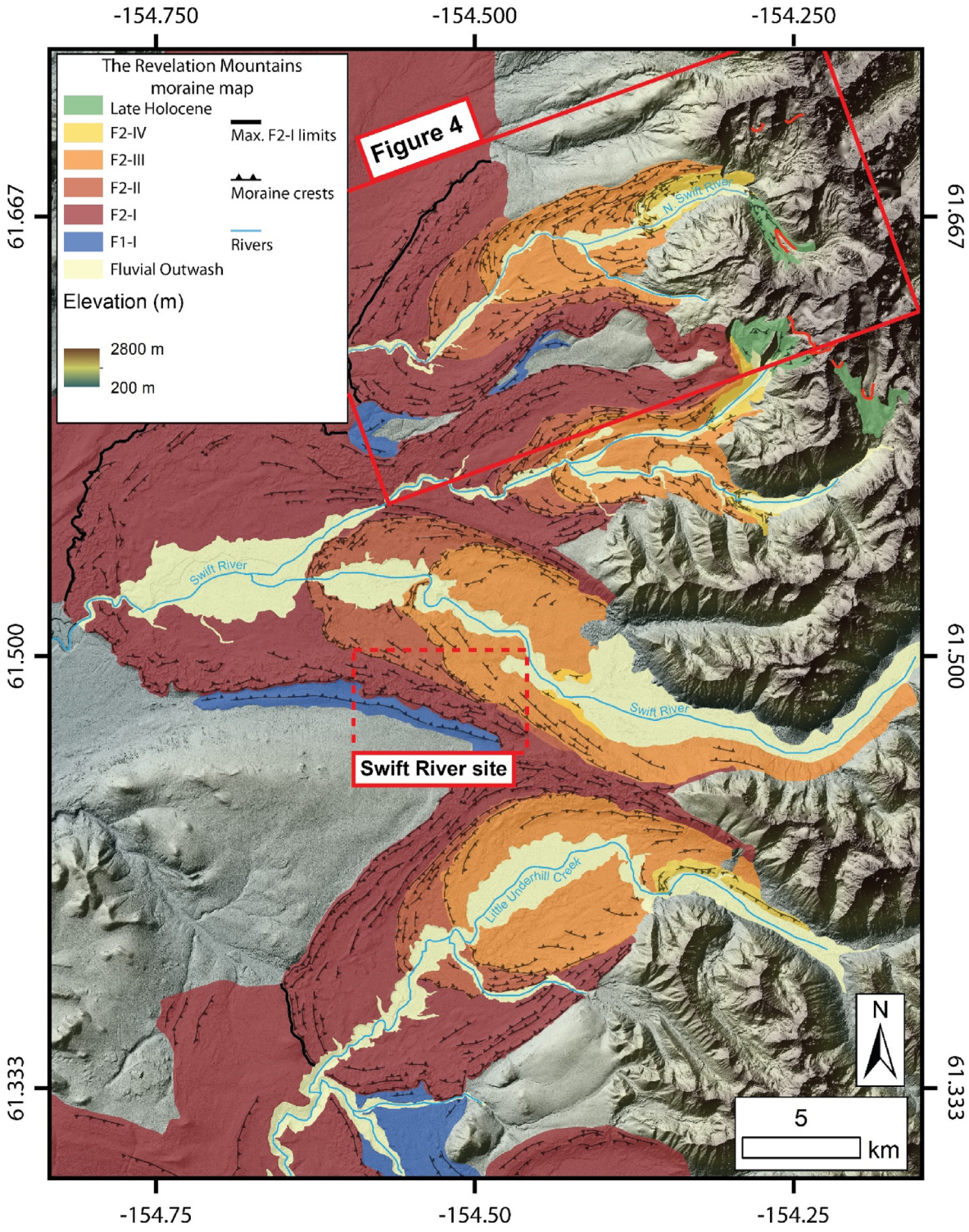

Fig. 3. Moraine map of the Revelation Mountains. Shaded relief overlain onto a DEM made available through the Polar Geospatial Center's Arctic DEM (https://www.pgc.umn.edu/data/arcticdem/). The four-fold sequence of moraines mapped here for the LGM and deglaciation (F2-I – F2-IV) follows the four-fold pattern observed elsewhere across the Alaska Range (Porter et al., 1983; Ten Brink and Waythomas, 1985; Kline and Bundtzen, 1986; Kaufman and Manley, 2004). As noted by mapped moraine crests across the Revelation Mountains, there are additional moraines preserved within the traditionally mapped four-fold units at this site. Local valley glaciers in the Revelation Mountains abutted up to large ice lobes flowing from the north and south during the LGM, and the thick black lines (Max. F2–I limits) denote the separation of deposits sourced from the Revelation Mountains and deposits from the large ice lobes.

Dryas. Of those that do, for example the Muldrow Glacier in the Alaska Range and the Waskey Mountain moraines, geomorphic evidence suggests these advances were extremely minor (less than 10% LGM length extents) and did not extend far from advances that occurred during the Holocene. It remains unknown how many other valleys across Alaska preserve Younger Dryas moraines. If there are other valleys that do contain Younger Dryas-age moraines, those moraines may similarly reside just outboard of late Holocene moraines since Younger Dryas advances, where evidence exists, appear to be quite minor across Alaska. To summarize, there is evidence suggesting that glaciers in Alaska – outside the Brooks Range – may have paused in their retreat through the last deglaciation around ca. 16–15 ka and ca. 13–12.5 ka, and evidence suggests these advances were somewhat limited at 40–30% and less than 10% of LGM length extents, respectively.

3. The Revelation Mountains

Kline and Bundtzen (1986) describe moraine sequences west of Denali National Park deposited during the last glacial cycle and locally refer to this glaciation as the Farewell Glaciation. They mapped deposits from the LGM and subsequent deglaciation as a four-fold sequence of Farewell 2 deposits (Farewell 1 being the penultimate, early Wisconsinan glaciation), based on moraine morphology and geographic positioning of the moraines. Furthermore, the four-fold Farewell 2 sequence is generally modeled after and correlated with the four-fold McKinley sequence mapped in Denali National Park (Ten Brink and Waythomas, 1985; Werner et al., 1993; Child, 1995), as well as in other valleys mapped across the Alaska Range (Porter et al., 1983; Kaufman and Manley, 2004). Farther south of where the Farewell Glaciation was first described, numerous alpine glaciers flowed westward from the Revelation Mountains of the western Alaska Range (Fig. 1 location 8: Fig. 3). Tulenko et al. (2018) adopted the Farewell nomenclature for the Revelation Mountains, and mapped moraine limits of LGM and deglaciation deposits based on moraine morphology and geographic positioning of the moraines, following the four-fold Farewell 2 sequence from Kline and Bundtzen (1986). The Revelation Mountains site had been previously surveyed in Briner et al. (2005), but had not yet been mapped in detail, so the adoption of the Farewell nomenclature was based on proximity to the nearest site in Alaska that had been formally mapped. Thus, we apply the nomenclature for the four-fold sequence to the moraines we mapped in detail in the Revelation Mountains in Tulenko et al. (2018) and this study, which are F2–I through F2-IV ("Farewell 2, one through four").

With more than two decades of glacial-geologic mapping and cosmogenic exposure dating across Alaska, we suggest that valleys draining the western Revelation Mountains provide one of the best opportunities in the state, perhaps the high northern latitudes, for exposure dating an alpine moraine chronology spanning the last deglaciation. These valleys contain (a) a high number of moraines up valley of the LGM terminal moraine (Figs. 3 and 4), and (b) the highest density of large boulders embedded in moraine crests than any other we are aware of. Moreover, the Revelation Mountains are comprised of plutonic granitic bedrock units of the McKinley sequence (ca. 57 Ma; Lanphere and Reed, 1985), and large boulders have been scoured, carried, and deposited by glaciers into the lowlands to the west throughout the Pleistocene. These boulders provide excellent targets for ^{10}Be dating because they are large, abundant, and contain quartz. The Revelation Mountains field site is approximately 55 km south of the western limb of the Denali Fault, which implies that this site may not have experienced as severe seismic activity as other valleys in the Alaska Range through the late Pleistocene. All said, the Revelation Mountains host relatively stable, dense moraine sequences with ample large granitic boulders, which are all crucial requirements for reconstructing reliable alpine glacier histories from direct constraints using ^{10}Be dating.

The first chronologic constraints for the Revelation Mountains come from the Swift River valley (Fig. 3) and constrain the timing of LGM culmination and initial deglaciation (Briner et al., 2005;

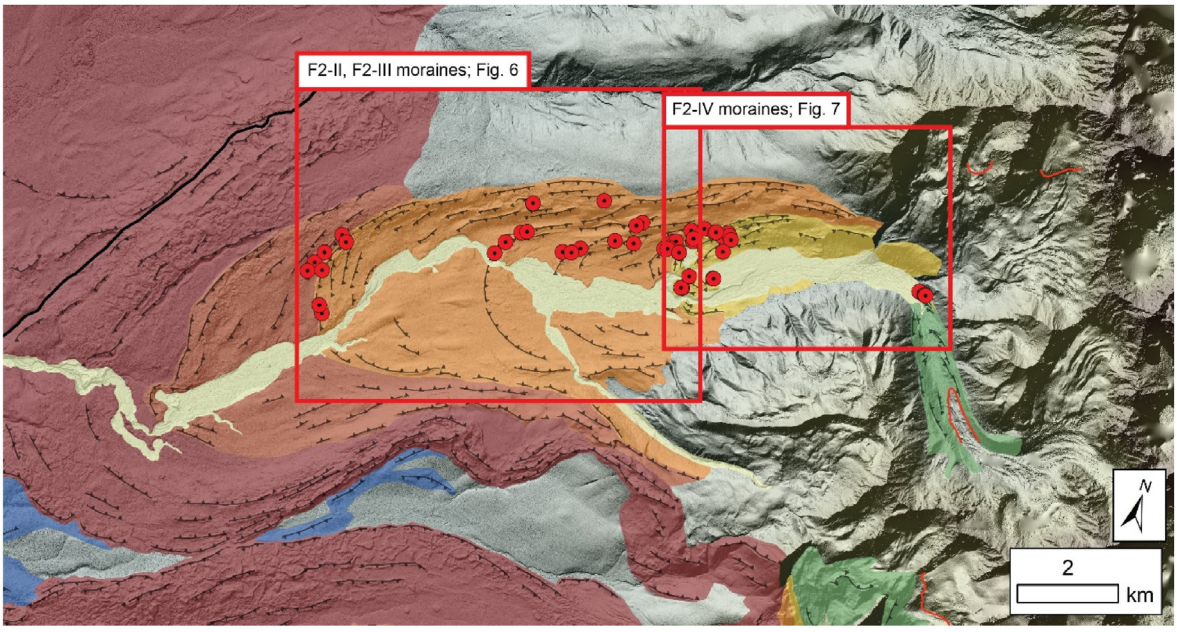

Fig. 4. The North Swift River valley field site. Locations of samples presented in this paper are highlighted with red circles. Fig. 6 (F2-II, F2-III moraines) and 7 (F2-IV moraines) are outlined in red boxes. Refer to Fig. 3 for explanation of map symbols. (For interpretation of the references to color in this figure legend, the reader is referred to the Web version of this article.)

Fig. 5. Field photos of a few large, quartz-rich boulders sampled in the North Swift River valley.

Tulenko et al., 2018). Here, surface samples were collected from moraine boulders deposited in the North Swift River valley (Fig. 4) north of the Swift River site (Fig. 3). The detailed sequence of moraines in the North Swift River valley is more condensed and easily accessible compared to the Swift River valley, and we were able to date 50 samples from boulders deposited on 11 distinct moraine crests. The new chronology is overlapped with the dataset published in Tulenko et al. (2018) — as opposed to combining for a single, composite record - to construct a master chronology of alpine glacier retreat through the last deglaciation in the Revelation Mountains.

4. Methods

4.1. Sample collection, processing, and measurements

Samples in the North Swift River valley were collected in the summer of 2019. Based on previous mapping and correlations across the Revelation Mountains (Tulenko et al., 2018), large granitic boulders on moraines were targeted from inside the F2-II limit up valley to an F2-IV moraine deposited just outside the mapped late Holocene moraines (Figs. 4 and 5). We specifically targeted large boulders situated directly on moraine crests to minimize the influence of post-depositional influence on ^{10}Be ages, which can be a significant issue plaguing the exposure dating of moraines in Alaska (Briner et al., 2005; Dortch et al., 2010a, 2010b; Valentino et al., 2021). Surface samples ranging from 1 to 3 cm in average thickness were collected using a battery-powered angle grinder and a hammer and chisel. We sampled flat, near-horizontal surfaces and avoided weathering pits to minimize the impact of boulder surface erosion on ^{10}Be ages.

Samples were processed at the University at Buffalo Cosmogenic Isotope Lab following the procedures outlined in Kohl and Nishiizumi (1992) for quartz extraction and in Corbett et al. (2016) for ^{10}Be isolation. Following crushing and sieving, a froth flotation method was used to isolate quartz-rich fractions from remaining minerals. Quartz-rich fractions were etched in low concentrations of HF/HNO_3 solutions until pure quartz was completely isolated. Samples were then analyzed for quartz purity via ICP-OES at the SUNY College of Environmental Science and Forestry. Following successful quartz purification, samples were dissolved in concentrated HF with a ^{9}Be spike in seven sample batches, each with a process blank. Be from each sample was isolated via ion exchange chromatography, and oxidized Be powder was packed into AMS cathodes. Samples were sent to the Purdue Rare Isotope Measurement Lab (PRIME Lab) for ^{10}Be/^{9}Be ratio AMS measurements, except for samples 19AK-60, 19AK-61, 19AK-62, 19AK-63, and 19AK-64, which were measured at the Center for Mass Spectrometry at Lawrence Livermore National Lab. Process blank ^{10}Be/^{9}Be ratios measured for each batch of samples are 1.97E-15, 3.14E-15, 2.69E-15, 2.00E-15, 3.12E-15, 1.40E-15, and 7.50E −16, and each sample is corrected for background ^{10}Be based on its respective process blank ratio (see Table 2 for process blank ratios corresponding to specific samples).

Table 2
^{10}Be ages from the North Swift River valley. Notes: Rock density for all samples assumed to be 2.65 g/cm^2. The Be standard used for AMS measurements is 07KNSTD. [1]Ages calculated using the Arctic PR (Young et al., 2013) and Lm scaling (Lal, 1991; Stone, 2000). [2]Ages calculated using the default production rate from CRONUS (Borchers et al., 2016) and Lm scaling (Lal, 1991; Stone, 2000). *Sample ^{10}Be/^{9}Be ratios measured at Lawrence Livermore National Laboratory. All remaining samples measured at PRIME Laboratory. Note that sample names in the table are the same as in Figs. 6 and 7 but have the 19AK prefix added.

Sample name	Latitude (DD)	Longitude (DD)	elevation (masl)	Shielding correction	Thickness (cm)	[Be-10] (atoms g-1)	+/− (atoms g-1)	Blank ratio	Age (ka)[1]	Age (ka)[2]
F2-II B										
19AK-02	61.65533	−154.49962	676	1.00000	3.0	153724	5838	3.14 E −15	19.0 ± 0.7	18.2 ± 0.7
19AK-03	61.65146	−154.50387	645	1.00000	1.5	128330	6145	3.14 E −15	16.1 ± 0.8	15.4 ± 0.7
19AK-04	61.64925	−154.50624	625	1.00000	2.0	142865	4237	1.97 E −15	18.3 ± 0.5	17.6 ± 0.5
19AK-05	61.64743	−154.50781	611	1.00000	2.0	145874	4008	1.97 E −15	18.9 ± 0.5	18.2 ± 0.5
F2-III A										
19AK-07	61.64103	−154.49777	582	1.00000	2.0	134486	4407	2.00 E −15	17.9 ± 0.6	17.2 ± 0.6
19AK-08	61.64226	−154.49963	586	1.00000	2.0	127997	4741	2.00 E −15	17.0 ± 0.6	16.3 ± 0.6
19AK-09	61.64832	−154.50267	617	1.00000	2.0	138626	4497	2.00 E −15	17.9 ± 0.6	17.2 ± 0.6
19AK-11	61.65436	−154.49736	645	1.00000	2.0	125470	4555	2.00 E −15	15.8 ± 0.6	15.2 ± 0.6
19AK-22	61.67096	−154.43503	714	1.00000	2.0	145968	4760	2.00 E −15	17.3 ± 0.6	16.6 ± 0.5
19AK-23	61.67106	−154.43515	714	1.00000	2.0	141496	5135	2.00 E −15	16.7 ± 0.6	16.1 ± 0.6
19AK-24	61.67530	−154.40993	783	1.00000	1.5	137905	5185	2.00 E −15	15.3 ± 0.6	14.7 ± 0.6
F2-III B										
19AK-15	61.66058	−154.44310	621	1.00000	2.0	153877	4826	2.00 E −15	19.8 ± 0.6	19.0 ± 0.6
19AK-18	61.66299	−154.44044	629	1.00000	2.0	126610	5035	3.12 E −15	16.2 ± 0.6	15.5 ± 0.6
19AK-19	61.66547	−154.43596	637	1.00000	3.0	121587	4518	3.12 E −15	15.5 ± 0.6	14.9 ± 0.6
19AK-20	61.66592	−154.43393	646	1.00000	2.0	134019	4868	3.12 E −15	16.9 ± 0.6	16.2 ± 0.6
19AK-25	61.67370	−154.39374	764	1.00000	2.0	136588	4632	3.12 E −15	15.5 ± 0.5	14.8 ± 0.5
19AK-26	61.67290	−154.39555	754	1.00000	3.0	205942	5899	3.12 E −15	23.7 ± 0.7	22.7 ± 0.7
F2-III C										
19AK-27	61.66974	−154.39450	705	1.00000	1.0	98297	3992	3.12 E −15	11.6 ± 0.5	11.1 ± 0.5
19AK-28	61.66915	−154.40146	699	1.00000	2.0	131333	5768	3.12 E −15	15.8 ± 0.7	15.1 ± 0.7
19AK-29	61.66598	−154.41292	659	1.00000	2.0	129236	5606	3.12 E −15	16.1 ± 0.7	15.4 ± 0.7
19AK-30	61.66482	−154.41571	652	1.00000	1.5	226638	6492	3.12 E −15	28.3 ± 0.8	27.1 ± 0.8
19AK-31	61.66442	−154.41888	637	1.00000	1.0	120903	4416	2.00 E −15	15.2 ± 0.6	14.6 ± 0.5
19AK-32	61.67501	−154.37535	755	1.00000	1.5	146548	7453	3.12 E −15	16.7 ± 0.9	16.0 ± 0.8
19AK-33	61.67601	−154.37086	770	1.00000	3.0	247273	6066	1.97 E −15	28.1 ± 0.7	26.9 ± 0.7
F2-III D										
19AK-45	61.67212	−154.38071	707	1.00000	1.5	139724	6000	3.14 E −15	16.6 ± 0.7	15.9 ± 0.7
19AK-50	61.67048	−154.38295	690	1.00000	2.0	137808	4704	3.14 E −15	16.7 ± 0.6	16.0 ± 0.5
F2-III E										
19AK-44	61.67239	−154.37958	710	1.00000	2.0	128482	4107	2.69 E −15	15.3 ± 0.5	14.6 ± 0.5
19AK-47	61.67098	−154.38150	697	1.00000	2.0	131541	4521	2.69 E −15	15.8 ± 0.5	15.2 ± 0.5
19AK-49	61.67065	−154.38179	693	1.00000	2.0	131958	4255	2.69 E −15	15.9 ± 0.5	15.3 ± 0.5
F2-IV A										
19AK-42	61.67375	−154.37364	736	1.00000	2.0	132565	5046	1.40 E −15	15.4 ± 0.6	14.8 ± 0.6
19AK-58	61.67061	−154.37724	704	1.00000	2.0	139240	4852	1.40 E −15	16.6 ± 0.6	15.9 ± 0.6
19AK-59	61.67066	−154.37720	704	1.00000	2.0	137500	5000	1.40 E −15	16.4 ± 0.6	15.7 ± 0.6
F2-IV B										
19AK-40	61.67590	−154.36664	758	1.00000	2.0	135336	5473	3.12 E −15	15.4 ± 0.6	14.8 ± 0.6
19AK-41	61.67607	−154.36630	760	1.00000	2.0	131494	5683	1.40 E −15	14.9 ± 0.6	14.3 ± 0.6
19AK-43	61.67331	−154.37357	728	1.00000	2.0	132695	3447	2.69 E −15	15.5 ± 0.4	14.9 ± 0.4
19AK-56	61.66484	−154.37204	698	1.00000	2.0	121929	4476	2.00 E −15	14.6 ± 0.5	14.0 ± 0.5
19AK-57	61.66484	−154.37244	699	1.00000	1.3	123476	4596	2.00 E −15	14.7 ± 0.6	14.1 ± 0.5
F2-IV C										
19AK-37	61.67662	−154.36179	764	1.00000	3.5	155020	4458	2.69 E −15	17.8 ± 0.5	17.0 ± 0.5
19AK-38	61.67574	−154.36369	751	1.00000	2.0	133130	3409	2.69 E −15	15.2 ± 0.4	14.6 ± 0.4
19AK-52	61.66811	−154.36209	704	1.00000	0.5	172667	5716	1.40 E −15	20.4 ± 0.7	19.5 ± 0.7
19AK-53	61.66814	−154.36186	704	1.00000	2.0	132589	4914	1.40 E −15	15.8 ± 0.6	15.2 ± 0.6
19AK-54	61.66720	−154.37088	700	1.00000	1.5	114866	4396	1.40 E −15	13.7 ± 0.5	13.1 ± 0.5
F2-IV D										
19AK-34	61.67619	−154.36110	758	1.00000	2.0	140303	5223	1.40 E −15	16.0 ± 0.6	15.3 ± 0.6
19AK-36	61.67558	−154.36012	745	1.00000	2.0	132360	4735	1.40 E −15	15.2 ± 0.5	14.6 ± 0.5
19AK-51	61.67316	−154.36163	704	1.00000	2.0	132076	4756	1.40 E −15	15.8 ± 0.6	15.1 ± 0.5
F2-IV E										
19AK-60[a]	61.67704	−154.28690	798	0.96805	1.9	116397	2173	7.50 E −16	13.2 ± 0.2	12.6 ± 0.2
19AK-61[a]	61.67677	−154.28461	822	0.96805	1.6	116890	1893	7.50 E −16	12.9 ± 0.2	12.4 ± 0.2
19AK-62[a]	61.67674	−154.28441	822	0.96805	2.7	114858	2143	7.50 E −16	12.8 ± 0.2	12.3 ± 0.2
19AK-63[a]	61.67680	−154.28427	822	0.96805	2.4	113519	2602	7.50 E −16	12.6 ± 0.3	12.1 ± 0.3
19AK-64[a]	61.67670	−154.28415	822	0.96805	3.1	110186	1778	7.50 E −16	12.3 ± 0.2	11.8 ± 0.2

4.2. Beryllium-10 age calculations

Beryllium-10 ages were calculated using version 3 of the online exposure age calculator (https://hess.ess.washington.edu/). Ages are calculated using the Arctic production rate (referred to hereafter as Arctic PR) of Young et al. (2013) and the Lal/Stone scaling scheme (referred to hereafter as Lm; Lal, 1991; Stone, 2000) to be consistent with calculations used at other sites across Alaska (Pendleton et al., 2015; Briner et al., 2017; Tulenko et al., 2018; Valentino et al., 2021). Additionally, ages are reported using the

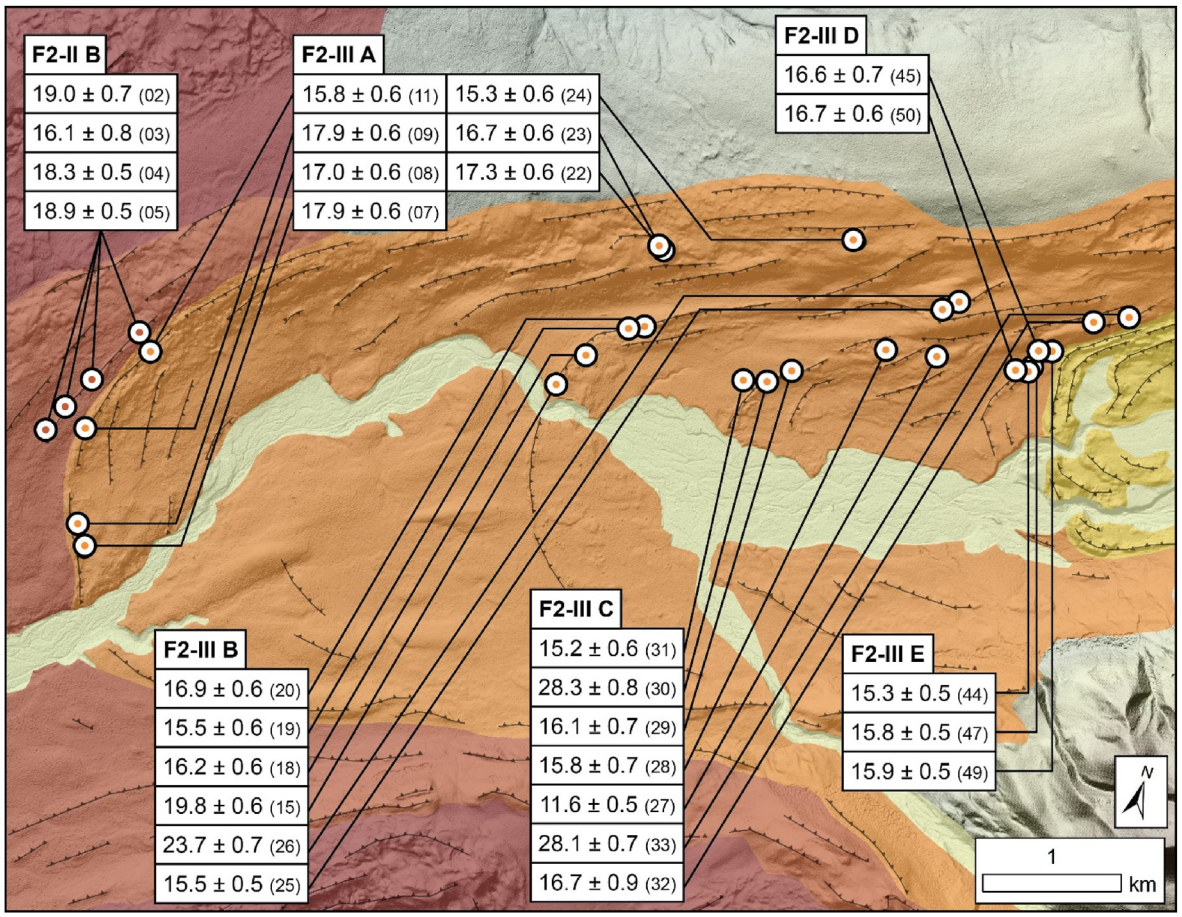

Fig. 6. Individual boulder ages for F2-II and F2-III moraines. Ages are reported with their 1σ analytical uncertainties. Sample numbers are reported in parentheses (note omitted "19AK" prefix for each sample that is seen in Table 2). Refer to Fig. 3 for explanation of map symbols.

default production rate from CRONUS (Borchers et al., 2016) in Table 2, but interpretations made throughout this manuscript are based on ages calculated using the Arctic PR/Lm scaling combination. Ages are not corrected for snow/sediment shielding, nor do we attempt to make corrections for boulder surface erosion. A rock density of 2.65 g/cm^3 is assumed for all samples.

Ages of each individual moraine are determined by calculating the mean and 1σ of the boulder ages from each moraine and exclude samples as outliers that do not overlap (i.e., are outside 2σ of the mean moraine age) with other ages from a moraine. Additional uncertainty is propagated through and added to each average moraine age uncertainty based on the empirically derived, 3.7% production rate uncertainty for the Arctic reported in Young et al. (2013).

5. Results

We present the average ages for the 11 distinct moraines based on the 50 ^{10}Be ages produced (Figs. 4, 6 and 7). One moraine crest is within the F2-II limit (F2-II B), five moraine crests are within the F2-III limit (F2-III A − E), and five crests are within the F2-IV limit (F2-IV A − E). See Figs. 3, 4, 6–10 for a visual description of units described in this section and note that we did not sample from moraines within the F2–I limit in the North Fork Swift River valley.

Beginning with the outermost moraine dated in the North Fork Swift River valley, ages from the F2-II moraine range from 19.0 ± 0.7–16.1 ± 0.8 ka (n = 4). Excluding one young outlier, ages suggest the F2-II B moraine was emplaced at 18.7 ± 0.8 ka.

Ages from the F2-III moraine package (five moraines, A − E) range from 28.3 ± 0.8–11.6 ± 0.5 ka (n = 25; Fig. 6). Excluding five likely outliers (four that are too old and one that is too young), ages suggest that F2-III A was emplaced at 16.9 ± 1.2 ka (n = 7), F2-III B was emplaced at 16.0 ± 0.9 ka (n = 4), F2-III C was emplaced at 15.9 ± 0.9 ka (n = 4), F2-III D was emplaced at 16.6 ± 0.6 ka (n = 2), and F2-III E was emplaced at 15.7 ± 0.7 ka (n = 3).

Ages from the F2-IV moraine package (5 moraines, A − E) range 20.4 ± 0.7–12.3 ± 0.2 ka (n = 21; Fig. 7). Excluding three likely outliers (two that are too old and one that is too young), ages suggest that F2-IV A was emplaced at 16.1 ± 0.9 ka (n = 3), F2-IV B was emplaced at 15.0 ± 0.7 ka (n = 5), F2-IV C was emplaced at 15.5 ± 0.7 ka (n = 2), F2-IV D was emplaced at 15.7 ± 0.7 ka (n = 3), and F2-IV E was emplaced at 12.8 ± 0.6 ka (n = 5).

6. Discussion

6.1. Reliability of moraine ages and the last deglaciation of the Revelation Mountains

In general, North Swift River valley moraine ages are in order according to their respective geographic positions down valley (Figs. 8–10). We also find, however, some boulder ages (n = 10; 20% of the dataset) that are statistical outliers, due either to isotopic inheritance for ages too old or post-depositional disruption for ages too young. These ages are outside of two standard deviations from calculated moraine ages and are thus rejected as outliers.

Moraine ages from mapped units correlated across the North

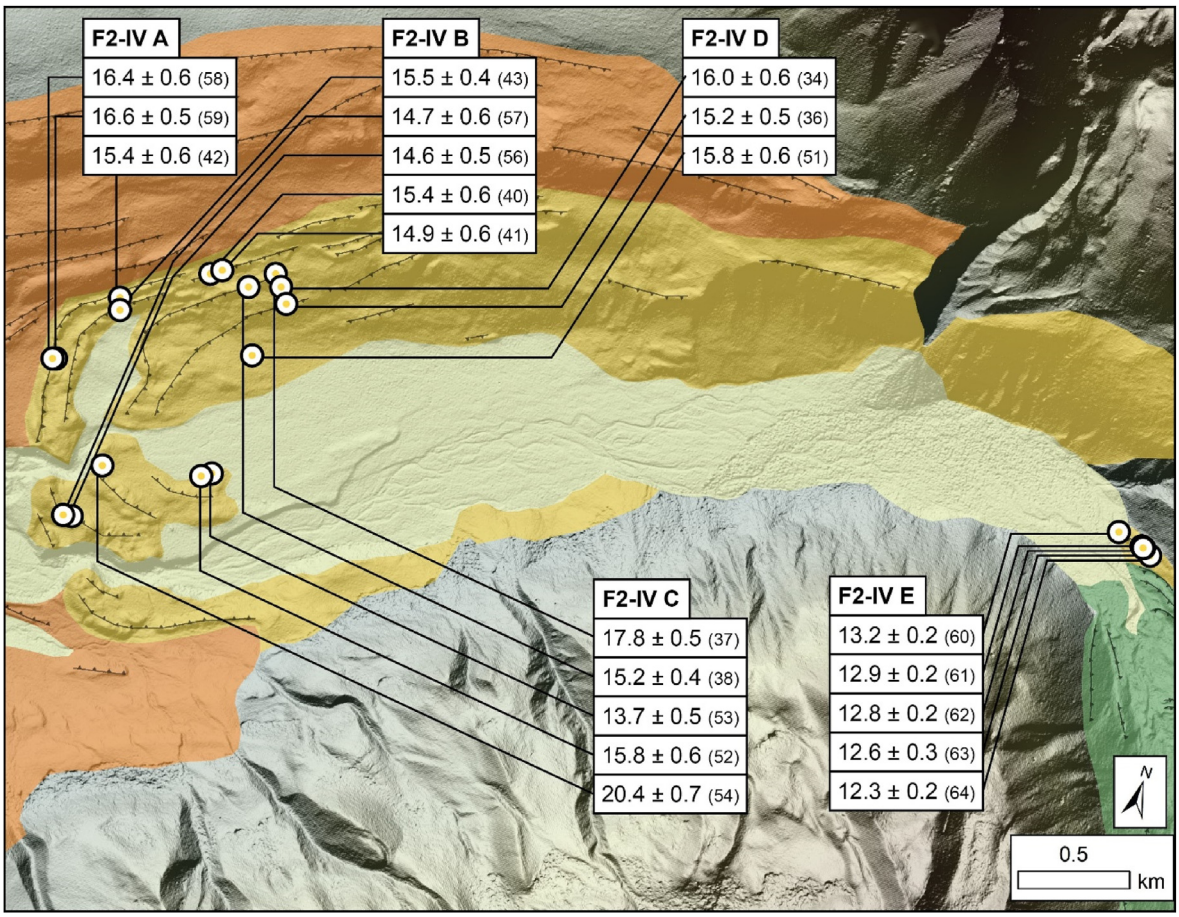

Fig. 7. Individual boulder ages for F2-IV moraines. Ages are reported with their 1σ analytical uncertainties. Sample numbers are reported in parentheses (note omitted "19AK" prefix for each sample that is seen in Table 2). Refer to Fig. 3 for explanation of map symbols. Note the late Holocene limits mapped in green just inboard of the F2-IV E moraine that are referenced later in the text. (For interpretation of the references to color in this figure legend, the reader is referred to the Web version of this article.)

Swift River valley and the Swift River valley appear to overlap; the F2-II B moraine age in the North Swift River valley at 18.7 ± 0.8 ka is between the F2-II A and F2-III A moraines dated in the Swift River valley at 19.5 ± 1.0 ka and 17.7 ± 0.9 ka, respectively. Furthermore, the F2-III A moraine dated in the North Swift River valley at 16.9 ± 1.2 ka overlaps with the F2-III A moraine dated in the Swift River valley at 17.7 ± 0.9 ka. Since these ages appear to overlap well, we are confident in the mapped correlation of moraine units made across the Revelation Mountains. However, the presence of many more than four moraines per valley (particularly in the North Swift River valley) and lack of significant time gap between the four original map units, suggests that the previously used four-fold designation for Alaska Range moraine sequences should be revisited.

To consider the timing and pace of retreat for the Revelation Mountains field site, we overlap the chronologies from the Swift River valley and the North Swift River valley into a single, master time-distance diagram for the Revelation Mountains (Fig. 11). As summarized in Tulenko et al. (2018), we found that the LGM culminated in the Revelation Mountains at 21.3 ka, with steady retreat until 17.7 ka. The North Swift River chronology indicates recession continued after emplacement of a moraine at 16.9 ka – mapped at the same extent as the 17.7 ka moraine in the Swift River valley – until recession stalled (or the glacier re-advanced) and the glacier deposited six moraines at approximately 30% of the valley length from LGM terminus to the modern glacier toe between ca. 16–15 ka. Here, the modern glacier toe is defined from aerial photo imagery collected in 1954 and catalogued in Earth Explorer (https://earthexplorer.usgs.gov/). Further recession followed this period of moraine deposition until the glacier deposited a moraine within 0.5 km of late Holocene moraines in the valley (see green mapped glacier limits and moraine crests in Fig. 7) at 12.8 ka (ca. 5% of the valley length from LGM terminus to the 1954 glacier extent). Any subsequent glacier fluctuations would have occurred within the limits of the late Holocene maximum extent, indicating that no other cold and/or wet periods sufficient to cause observable re-advances occurred after 12.8 ka.

6.2. The last deglaciation of Alaska

Numerous sites across Alaska support parts of the reconstructed glacier history from the Revelation Mountains (Fig. 12). Most records available from Alaska indicate a culmination of the LGM between ca. 21–19 ka. The records summarized in the Brooks Range indicate glaciers underwent significant retreat between ca. 21–18 ka, and then following moraine deposition between ca. 18–17 ka, rapidly retreated into their cirques by ca. 15 ka. Across the Alaska Range, the collective records of glacier change indicate recession after ca. 19 ka, and a pause in deglaciation between ca. 16–15 ka, where multiple valleys have moraines dating within that period. This is especially true for the Revelation Mountains, where six distinct and tightly nested moraines were deposited between ca. 16–15 ka. Additionally, we note a few instances of moraines dating between 13 and 12 ka that are situated immediately outboard of

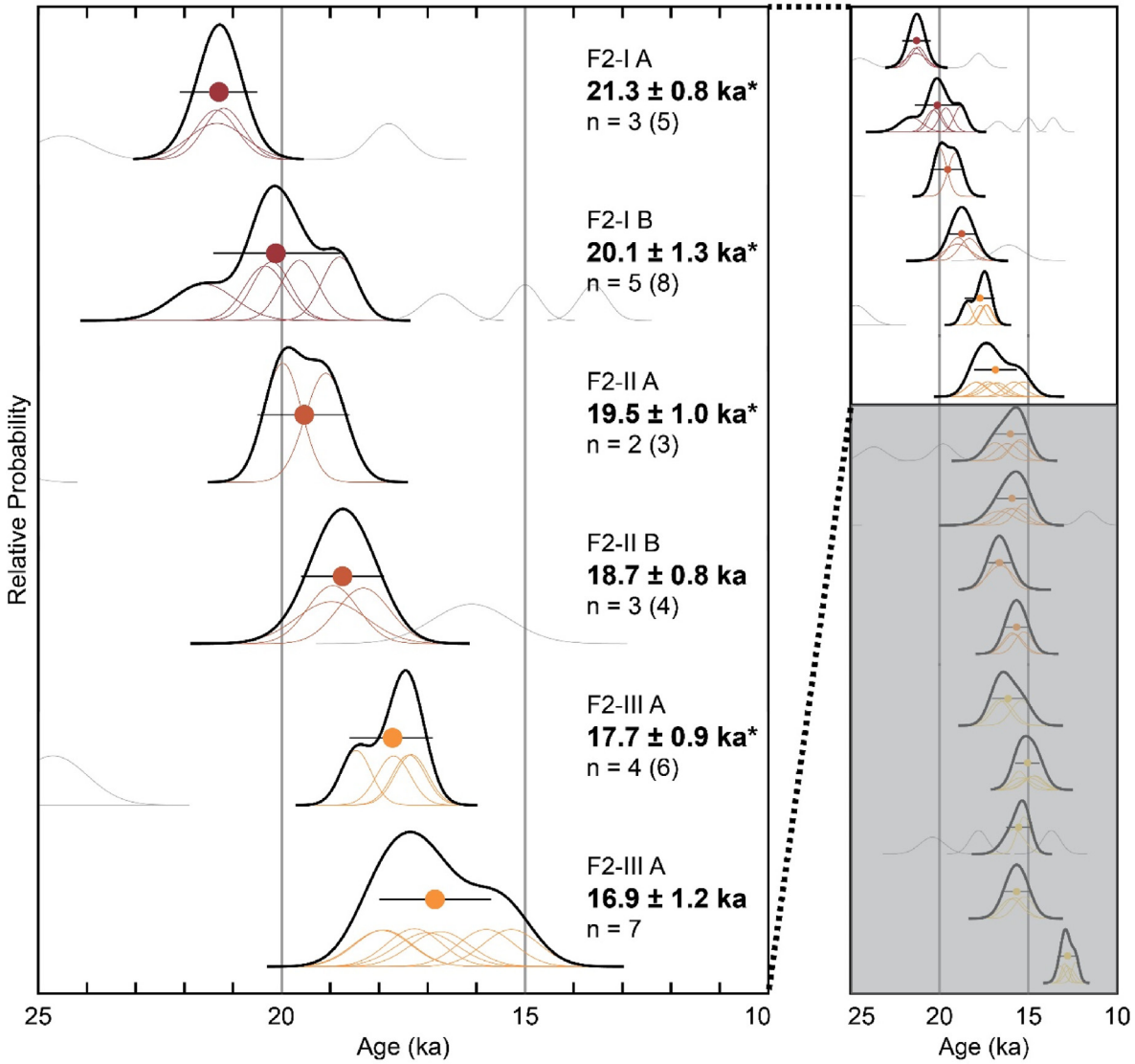

Fig. 8. Summed probability plots for F2−I, F2-II, and the outermost F2-III moraines. Moraine ages reported in the left plot with the * symbol are from the Swift River valley site (Tulenko et al., 2018, Fig. 3), and remaining moraine ages are from the North Swift River valley (this study). Ages in the left plot are an expanded view of the white area in the right plot. Note the right plot shows all summed probability plots for each moraine dated in the Revelation Mountains from Tulenko et al. (2018) and this study. Individual ages are normal distributions using the calculated age and measured analytical uncertainty for mean and 1σ. Moraine ages are reported as the mean and 1σ of the population of ages from each moraine (excluding likely outliers that are plotted in grey). Right plot shows summed probability curves for every moraine dated in the Revelation Mountains arranged in geographic position down valley.

late Holocene moraines. Farther south, in the Ahklun Mountains, chronologies indicate the LGM culminated ca. 21 ka, in-sync with glaciers in the rest of the state, with sustained recession at least until ca. 19 ka. The timing and rate of retreat through the deglacial period for the Ahklun Mountains remains poorly constrained, except for evidence of glacier advances ca. 12.5 and 12.1 ka.

6.3. Climate forcing of the last deglaciation of Alaska

We now compare records of alpine deglaciation across Alaska to other climate proxies outside the state to address what climatic factors may have been most important for driving glacier retreat through the last deglaciation (Fig. 13). We take a qualitative approach of observing the correlations and deviations between Alaska alpine glacier records and several global and regional climatic proxy records. We rely most heavily on our new record of retreat from the Revelation Mountains since the record is the most complete and spans the entire deglacial period.

It is likely that non-climatic factors played a role in some of the observed variations in response times and retreat rates of valley glaciers across Alaska following the LGM. For example, individual valley hypsometries across the state vary, which might influence the timing and rate of retreat in each valley. A more qualitative approach of reconstructing alpine glacier equilibrium line altitudes across the state to mitigate the effects of valley hypsometries and potentially highlight climate forcing would be a worthwhile future endeavor. Furthermore, glacial isostatic adjustment following deglaciation could theoretically lead to glacier stabilization in the region as slow (millennial-scale) landscape uplift leads to an increase in glacier elevations, effectively lowering glacier equilibrium line altitudes. However, model output of glacial isostatic adjustment following the LGM from ICE-6G (Peltier et al., 2015) indicates

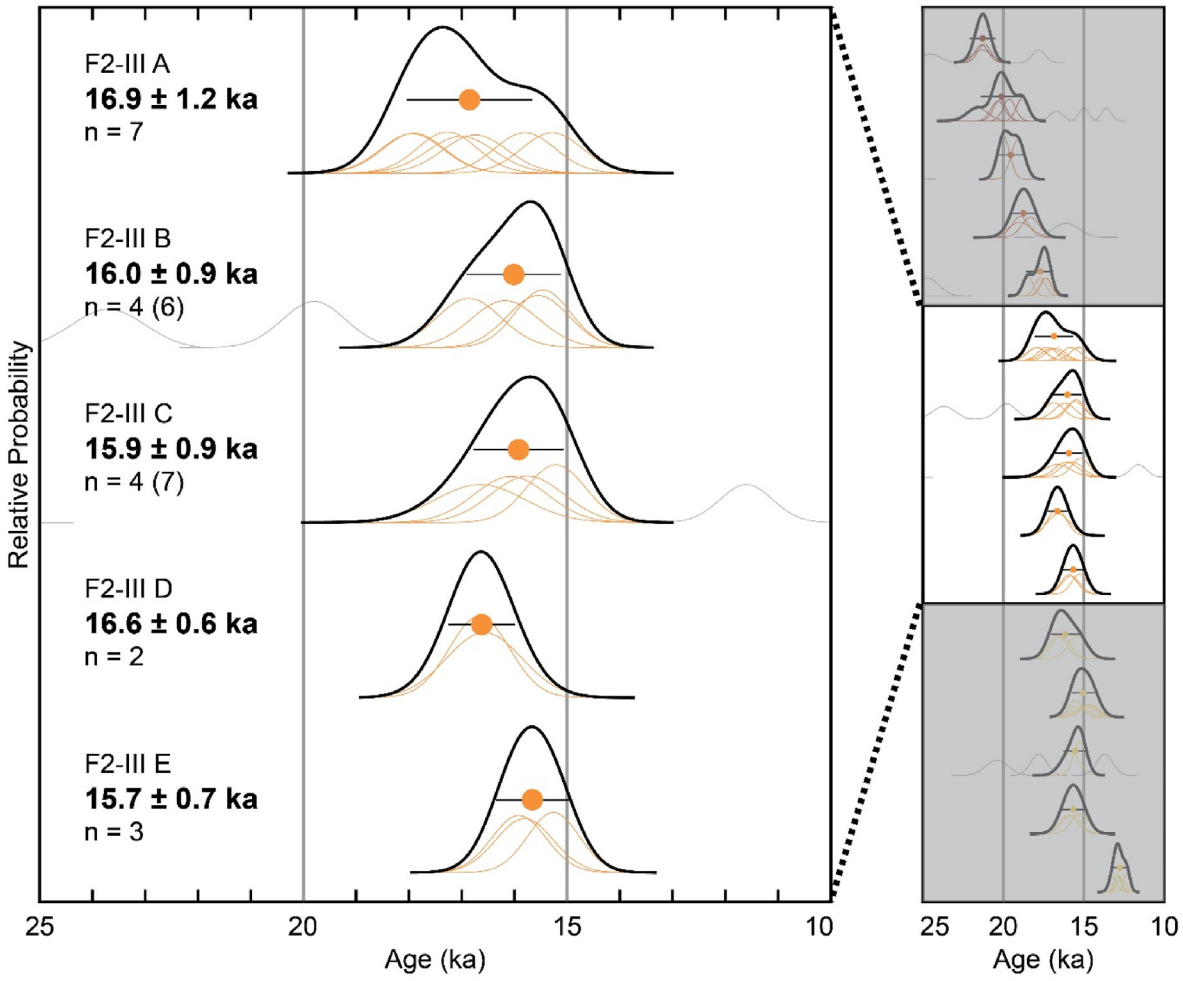

Fig. 9. Summed probability plots for F2-III moraines from the North Swift River valley. Moraine ages reported in the left plot are an expanded view of the white area in the right plot. Note the right plot shows all summed probability plots for each moraine dated in the Revelation Mountains from Tulenko et al. (2018) and this study. Individual ages are normal distributions using the calculated age and measured analytical uncertainty for mean and 1σ. Moraine ages are reported as the mean and 1σ of the population of ages from each moraine (excluding likely outliers that are plotted in grey). Right plot shows summed probability curves for every moraine dated in the Revelation Mountains arranged in geographic position down valley.

virtually no current glacial isostatic adjustment in Alaska outside Southeast Alaska. Additionally, modeled relative sea level curves from Southeast Alaska indicate ~125 m of glacial isostatic adjustment from the Cordilleran Ice Sheet, which fits observations (Andrews and Retherford, 1978) somewhat well; see Fig. 8 in Peltier et al. (2015) for more details. So, while glacial isostatic adjustment could play a role in some parts of Alaska, available evidence suggests that in interior Alaska, relatively minor uplift following deglaciation may not be a significant influence on glacier history.

If warming from rising Boreal summer insolation through the last deglaciation was the dominant forcing mechanism driving glacier retreat across Alaska, we would expect an Alaska-wide LGM culmination around the timing of an insolation minimum, steady retreat following, and then perhaps moraine deposition sometime after boreal summer insolation peaked and began decreasing again. Boreal (65° N) peak summer insolation reaches a local minimum and begins rising ca. 23–21 ka, reaches a local maximum in the early Holocene and begins decreasing through the Holocene (Laskar et al., 2004, Fig. 13). Our moraine record, and others across Alaska, indicate that glaciers culminated between 21 and 19 ka and began steadily retreating afterward. Furthermore, paleoclimate proxies from the Bering Sea indicate concomitant, steadily warming sea surface temperatures and reductions in sea ice cover also potentially in response to rising insolation (Caissie et al., 2010). However, our moraine record reveals periods of glacier stabilization and moraine deposition, particularly at ca. 16–15 ka and ca. 13–12 ka that might be unexpected if warming from rising boreal summer insolation was the dominant forcing mechanism. We suggest that while warming from rising boreal insolation may have influenced the timing of LGM culmination across Alaska and forced initial and thereafter steady deglaciation across the state, other climatic mechanisms may have dominated the overall pattern of retreat through the rest of the deglacial period.

If warming forced by rising global atmospheric CO_2 concentrations (hereafter referred to as global CO_2) was the main driver of alpine deglaciation in Alaska, we might expect glacier retreat to coincide with rising global CO_2 and perhaps several moraine deposition events occurring while global CO_2 was decreasing (i.e., during the Antarctic cold reversal; Pedro et al., 2016). Following the LGM, Antarctic ice core records indicate that global CO_2 did not begin rising until ca. 18 ka (Bereiter et al., 2015, Fig. 13). There are also a few intervals where global CO_2 levels off or decreases, namely from ca. 16–15 ka and during the Antarctic cold reversal between 14.7 and 13 ka (Pedro et al., 2011). In Alaska, the LGM culmination occurred at ca. 21–19 ka. Glacier records indicate as much as 30% net retreat prior to ca. 18 ka when global CO_2 began rising. It seems

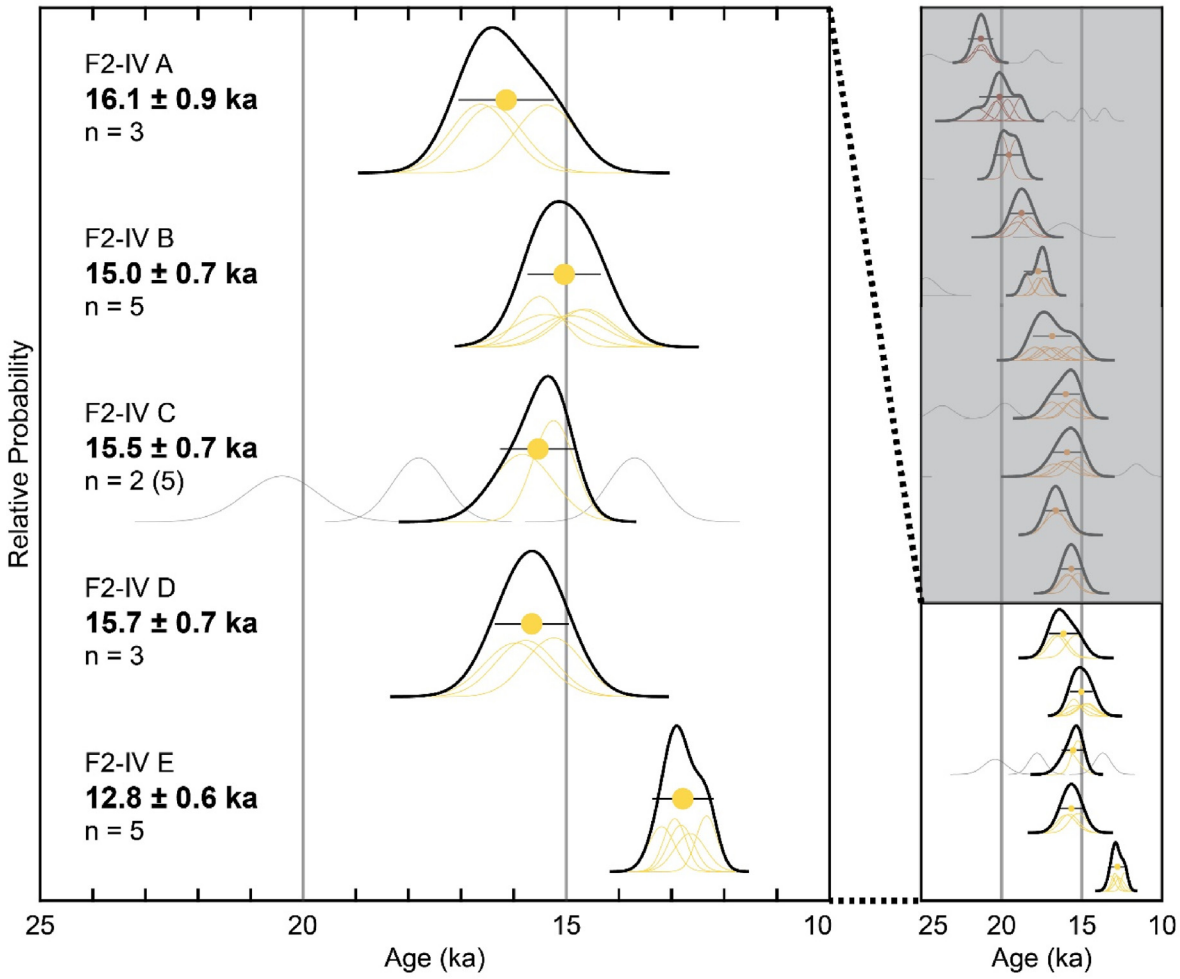

Fig. 10. Summed probability Plots for F2-IV moraines from the North Swift River valley. Moraine ages reported in the left plot are an expanded view of the white area in the right plot. Note the right plot shows all summed probability plots for each moraine dated in the Revelation Mountains from Tulenko et al. (2018) and this study. Individual ages are normal distributions using the calculated age and measured analytical uncertainty for mean and 1σ. Moraine ages are reported as the mean and 1σ of the population of ages from each moraine (excluding likely outliers that are plotted in grey). Right plot shows summed probability curves for every moraine dated in the Revelation Mountains arranged in geographic position down valley.

likely that this interval of retreat was not driven by global CO_2, but perhaps by rising insolation. However, we observe accelerated retreat between ca. 17–16 ka that is generally synchronous with the timing of global CO_2 rise (Fig. 13). We suggest that global CO_2 rise between ca. 17–16 ka may have forced additional warming that accelerated glacier retreat across Alaska over the same interval. Yet, late-glacial moraine deposition events observed across Alaska appear to be both in and out of phase with decreasing global CO_2 during ca. 16–15 ka and 13–12 ka, so it appears that after ca. 15 ka, other climatic forcing mechanisms became more important than global CO_2.

If changes to Northern Hemisphere ocean circulation that impacted climate records in other regions around the Northern Hemisphere [North Atlantic region; NGRIP members, 2004; North Pacific region; Praetorius et al. (2020), Asia; Wang et al. (2001)] significantly impacted alpine deglaciation across Alaska, we would expect the following pattern: glaciers would be expanded throughout Heinrich Stadial 1, glaciers would retreat through the Bølling/Allerød period, and glaciers would advance during some portion of the Younger Dryas. We observe that glaciers in the Revelation Mountains and across the rest of Alaska steadily retreated until the latter stages of Heinrich Stadial 1. However, there are notable periods of moraine deposition that coincide with the culmination of Heinrich Stadial 1 between ca. 16–15 ka, and during the early Younger Dryas cold period. We also note a period of rapid retreat and non-deposition between ca. 15–13 ka in the Revelation Mountains that roughly coincides with Bølling/Allerød warming. We suggest that because moraine deposition events coincide with observed trends towards colder temperatures in North Atlantic records, there must have been some influence of Northern Hemisphere Ocean circulation forcing on the deglacial pattern in Alaska.

The Bering Strait separating Alaska and eastern Siberia is shallow (ca. 53 m water depth; Jakobsson et al., 2017), was exposed during the LGM, and the transition from exposed to flooded occurred during the last deglaciation. This geologic event is often explored as a control on local climate in Beringia (Elias et al., 1996; Brigham-Grette, 2001; Daniels et al., 2021). If the flooding of the Bering Land Bridge and associated changes to moisture delivery and ocean circulation were responsible for driving the pattern of alpine deglaciation across the state, we would expect prominent glacier readvances/standstills ca. 13.4–11 ka as local sea level transgressed and the bridge became flooded (England and Furze, 2008; Jakobsson et al., 2017). Flooding potentially caused a

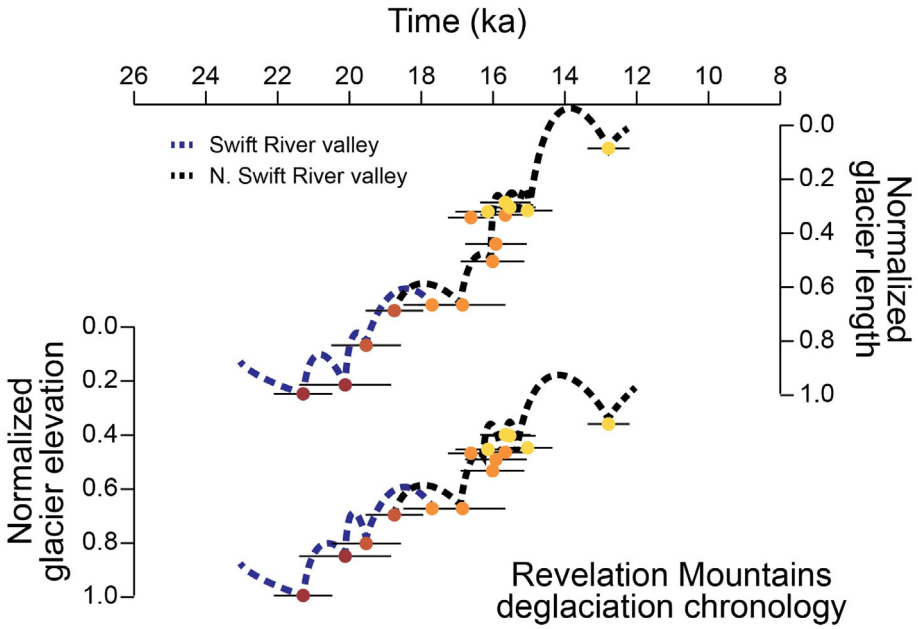

Fig. 11. Time-distance diagram of glaciers in the Revelation Mountains. Top plot is normalized by glacier length where 1 = LGM glacier length at the toe and 0 = modern (i.e., 1954) glacier length at the toe (total valley floor length = 25680 m). Bottom plot is normalized in the same way except by elevation, which ranges 540–940 m asl. Dashed lines represent a hypothetical pattern of glacier fluctuations through the last deglaciation if moraines were deposited during minor re-advances.

reduction in continentality in interior Alaska, increases in moisture delivery to the region and perhaps led to slight summer cooling/more temperate climate (Brigham-Grette, 2001; Daniels et al., 2021), all of which could support glacier growth. We do find statewide that while glaciers were significantly reduced relative to their LGM length extents, glaciers readvanced – or were in a standstill – ca. 13–12 ka, which coincides with the flooding of the Bering Land Bridge. We suggest that this may be an alternative explanation to why glaciers statewide were readvancing during this time period. However, it does not explain the timing and pace of glacier retreat through the entire deglacial period, especially prior to the timing of flooding since the Revelation Mountains glaciers had already retreated to within ~1 km of late Holocene extents by then. Furthermore, it is difficult to know if glaciers were responding over this interval to far-field Younger Dryas cooling or Bering Land Bridge flooding since both events occurred roughly at the same time.

Model simulations indicate that Alaska remained relatively warm and dry during the LGM possibly due to the re-organization of atmospheric circulation patterns driven by large, impeding North American ice sheets (COHMAP Members, 1988; Roe and Lindzen, 2001; Otto-Bliesner et al., 2006; Löfverström and Liakka, 2016; Liakka and Lofverstrom, 2018). Tulenko et al. (2020b) further hypothesizes that the various configurations of North American ice sheets over the last glacial cycle may have modulated regional climate and alpine glaciers leading to the somewhat unique pattern of alpine glacier moraine preservation across North America. Following a similar mechanism described in Tulenko et al. (2020b), model simulations suggest that through the last deglaciation, a major reorganization of atmospheric circulation patterns occurred directly after the separation of the Cordilleran and Laurentide ice sheets in a rapid, stepwise manner (Lora et al., 2016; Löfverström and Lora, 2017). In model simulations, the major impact of changing atmospheric circulation patterns involving the 'saddle collapse' between the Cordilleran and Laurentide ice sheets is that Alaska cooled, and the western United States warmed. Terrestrial data from interior Canada indicate that the saddle collapse geologic event occurred sometime between ca. 15.5–14 ka (Dalton et al., 2020). Indeed, terrestrial data across the western United States indicate that substantial warming, glacier retreat and pluvial lake lowering occurred abruptly, and around the time of the saddle collapse (Ibarra et al., 2014; Reheis et al., 2014; Lora and Ibarra, 2019; Tulenko et al., 2020a). If changing atmospheric circulation in response to the saddle collapse made a significant impact on the pattern of deglaciation in Alaska, we would expect a readvance/standstill of glaciers sometime between ca. 15.5–14 ka since atmospheric re-organization would result in cooling Alaska. We do observe advances/standstills across the state between ca. 16–15 ka, which may coincide with the saddle collapse. Thus, it is possible that ice sheet-induced atmospheric circulation is an alternative explanation for the timing of moraine emplacement during this time interval in Alaska. As with the flooding of the Bering Land Bridge, this mechanism would only explain one portion of the Revelation Mountains moraine record since atmospheric re-organization appears to have happened in a stepwise manner. Thus, it seems unlikely that the saddle collapse event impacted deglaciation in Alaska outside of the ~16–15 ka interval.

Following the LGM, paleoclimate proxies from the Bering Sea indicate steady reductions in sea ice cover and rising sea surface temperatures (Caissie et al., 2010). Sea ice-free conditions and warmer sea surface temperatures would likely increase moisture availability to interior Alaska, and increased precipitation could subsequently drive glacier stabilization. While it is possible that changing precipitation played a significant role stabilizing glaciers across Alaska – particularly around ~15 ka when there are coincident glacier readvances/stabilizations across Alaska and a transition from perennial sea ice cover to seasonal sea ice cover – seasonal sea ice cover would possibly inhibit moisture delivery in the winter in the same way that perennial sea ice cover does. Thus, since glaciers are most sensitive to summer temperatures and winter precipitation (snow/ice accumulation), perhaps sea ice cover changes would not influence glaciers as strongly as summer temperature at this time. Determining the changes in magnitude of wintertime moisture delivery to interior Alaska through the last

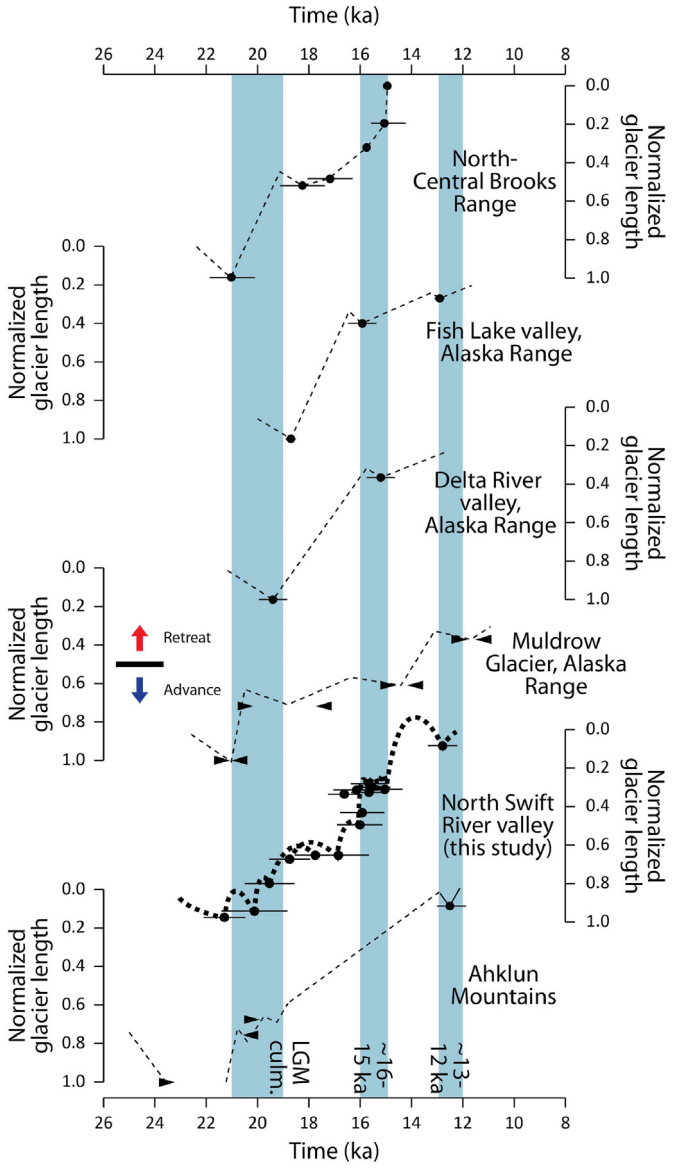

Fig. 12. Time-distance diagrams of glaciers in Alaska. Time-distance diagrams of alpine glacier retreat following the LGM from sites across Alaska summarized in this paper. Glacier lengths are normalized in the same way as in Fig. 11. Vertical blue bars represent periods of significant moraine-building events observed across the state. Dots with horizontal bars are average moraine ages from cosmogenic exposure ages and left and right triangles are minimum and maximum radiocarbon constraints, respectively, on moraine positions. From top to bottom: North-central Brooks Range (Pendleton et al., 2015); Fish Lake valley, AK Range (Young et al., 2009); Delta River valley, AK Range (Howley, 2008; Matmon et al., 2010); Muldrow Glacier, AK Range (Ten Brink and Waythomas, 1985; Werner et al., 1993; Child, 1995); Revelation Mountains (Tulenko et al., 2018; this study); Ahklun Mountains (Manley et al., 2001; Briner et al., 2002; Kaufman et al., 2003, 2012; Young et al., 2019). (For interpretation of the references to color in this figure legend, the reader is referred to the Web version of this article.)

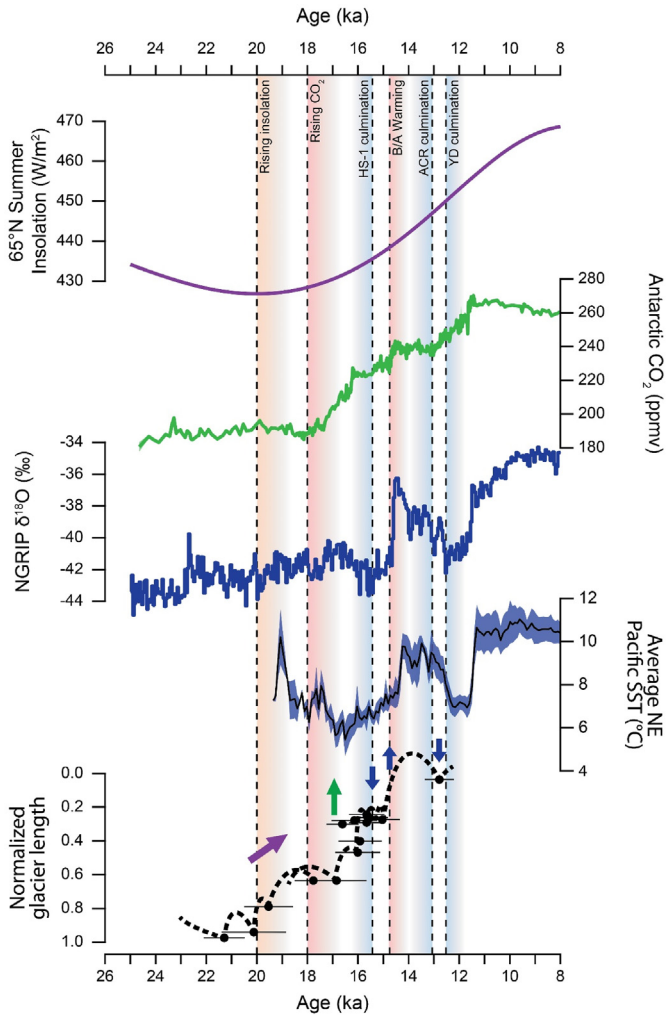

Fig. 13. Climate records compared to the Revelation Mountains chronology. From top to bottom; June insolation for 65° N (Laskar et al., 2004), Antarctic ice core CO_2 concentrations (Bereiter et al., 2015), NGRIP ice core $\delta^{18}O$ data (NGRIP members, 2004), average northeast Pacific Ocean SST's (Praetorius et al., 2020), and the master chronology of alpine glacier retreat from the Revelation Mountains from Fig. 11. Arrows indicate glacier fluctuations tied to color coded proxy records. Vertical dash marks followed by warm-colored bars indicate the onsets of warming from rising insolation, rising CO_2 and rising North-Atlantic temperature, and vertical dash marks preceded by cool-colored bars indicate the culminations of cold events (i.e., Heinrich Stadial 1, the Antarctic Cold Reversal, and the Younger Dryas). Readers are referred to the online version for color descriptions. (For interpretation of the references to color in this figure legend, the reader is referred to the Web version of this article.)

deglaciation would be an important test to determine how precipitation may have impacted glaciers in Alaska.

7. Conclusions

We provide a benchmark chronology of alpine glacier retreat from the Revelation Mountains of the western Alaska Range following the LGM and summarize the current state of knowledge of the timing and pace of alpine deglaciation across Alaska. Our chronology, along with a few other key chronologies, reveal a culmination of LGM alpine glacier advances across the state between ca. 21–19 ka. Post-LGM deglaciation initiated directly after ca. 21–19 ka, and the Revelation Mountains chronology reveals periods of accelerated retreat between ca. 17–16 ka and ca. 15–13 ka. Embedded within the overall pattern of retreat were periods of substantial moraine deposition, notably at ca. 16–15 ka and ca. 13–12 ka.

Climate proxy data and model simulations reveal a relatively mild LGM temperature depression of approximately 4 °C across Alaska, which would support the fact that much of interior Alaska remained ice-free and glaciation was restricted to high mountains across the state during the LGM. Following the LGM, there appears to be some asynchrony in the timing of warming, where proxy data suggests that warming in southern Alaska occurred immediately after the culmination of the LGM, while northern Alaska may have

remained relatively cold until ca. 17 ka. However, alpine glacier records indicate that glaciers throughout Alaska were retreating prior to ca. 17 ka. Some discrepancies between alpine glacier records and proxy data from the Brooks Range (e.g., Daniels et al., 2021) have yet to be resolved, although it is possible that the discrepancy has to do with seasonality and whether alpine glacier records and other proxy data are more heavily influenced by different seasonal climate.

Regarding the climate mechanisms that influenced the timing and pace of alpine deglaciation across the state, we compare glacier records to several global and regional climate proxy data. We find that initial deglaciation may have been driven by warming due to rising boreal insolation as it is the only mechanism identified that could lead to glacier recession prior to the onset of CO_2. However, after ca. 18 ka, we observe accelerated retreat of the Revelation Mountains that we attribute to additional warming forced by global CO_2 rise. We also find that alpine glacier retreat may have been influenced by high northern latitude stadial conditions reflected in records from the North Atlantic and North Pacific regions during the Bølling/Allerød period (Fig. 13). Periods of moraine deposition near the end of HS-1 and during the Younger Dryas cold period also indicate a possible teleconnection across the high northern latitudes between the North Atlantic region and Alaska-North Pacific region. Other possible mechanisms for periods of moraine deposition at ca. 16–15 ka and ca. 13–12 ka, such as ice sheet influence on regional atmospheric circulation, the flooding of the Bering Land Bridge, and Bering Sea moisture dynamics could still potentially explain these periods of moraine deposition. Alpine glacier chronologies across Alaska, including the new chronology from the Revelation Mountains reveal a complex response of high northern latitude glaciers to multiple forcings through the last deglaciation and underscore the likelihood of a complex response of remaining glaciers world-wide to future climate change.

Credit Author statement

Joseph P Tulenko: Conceptualization, Formal analysis, Investigation, Writing – Original Draft, Visualization. Jason P Briner: Conceptualization, Investigation, Writing – Review and Editing, Funding acquisition. Nicolás E Young: Conceptualization, Investigation, Writing – Review and Editing, Funding acquisition. Joerg M Schaefer: Conceptualization, Writing – Review and Editing, Funding acquisition.

Declaration of competing interest

The authors declare that they have no known competing financial interests or personal relationships that could have appeared to influence the work reported in this paper.

Acknowledgements

We would like to acknowledge that samples in this study were collected on ancestral lands of the Dënéndeh and Dena'ina Ełnena and that the University at Buffalo exists on the land of the Seneca. These peoples are the traditional caretakers of these lands. We give thanks for the opportunity to exist and work on lands that are rightfully theirs. We would like to thank Chris Sbarra and Brendan Ash for help with sample preparation. We also thank PRIME Lab and LLNL for AMS measurements. This projected was supported by NSF Grant no. 1853705. We would also like to thank Dr. Julie Brigham-Grette and one anonymous reviewer for their insightful and thorough reviews, both of which greatly strengthened this manuscript.

Appendix A. Supplementary data

Supplementary data to this article can be found online at https://doi.org/10.1016/j.quascirev.2022.107549.

References

Abbott, M.B., Edwards, M.E., Finney, B.P., 2010. A 40,000-yr record of environmental change from Burial Lake in Northwest Alaska. Quat. Res. 74, 156–165.

Andrews, J.T., Retherford, R.M., 1978. A reconnaissance survey of late Quaternary sea levels, Bella Bella/Bella Coola region, central British Columbia coast. Can. J. Earth Sci. 15, 341–350. https://doi.org/10.1139/e78-040.

Badding, M.E., Briner, J.P., Kaufman, D.S., 2013. ^{10}Be ages of late Pleistocene deglaciation and neoglaciation in the North-central Brooks range, Arctic Alaska. J. Quat. Sci. 28, 95–102. https://doi.org/10.1002/jqs.2596.

Balascio, N.L., Kaufman, D.S., Briner, J.P., Manley, W.F., 2005. Late Pleistocene glacial geology of the Okpilak-Kongakut rivers region, northeastern Brooks Range, Alaska. Arctic Antarct. Alpine Res. 37, 416–424.

Barrell, D.J., Putnam, A.E., Denton, G.H., 2019. Reconciling the onset of deglaciation in the upper Rangitata valley, Southern Alps, New Zealand. Quat. Sci. Rev. 203, 141–150.

Bereiter, B., Eggleston, S., Schmitt, J., Nehrbass-Ahles, C., Stocker, T.F., Fischer, H., Kipfstuhl, S., Chappellaz, J., 2015. Revision of the EPICA Dome C CO_2 record from 800 to 600 kyr before present. Geophys. Res. Lett. 42, 542–549.

Borchers, B., Marrero, S., Balco, G., Caffee, M., Goehring, B., Lifton, N., Nishiizumi, K., Phillips, F., Schaefer, J., Stone, J., 2016. Geological calibration of spallation production rates in the CRONUS-Earth project. Quat. Geochronol. 31, 188–198.

Brigham-Grette, J., 2001. New perspectives on Beringian Quaternary paleogeography, stratigraphy, and glacial history. Quat. Sci. Rev. 20, 15–24. https://doi.org/10.1016/S0277-3791(00)00134-7.

Briner, J.P., Kaufman, D.S., Manley, W.F., Finkel, R.C., Caffee, M.W., 2005. Cosmogenic exposure dating of late Pleistocene moraine stabilization in Alaska. Geol. Soc. Am. Bull. 117, 1108–1120.

Briner, J.P., Kaufman, D.S., Werner, A., Caffee, M., Levy, L., Manley, W.F., Kaplan, M.R., Finkel, R.C., 2002. glacier readvance during the late glacial (younger Dryas?) in the Ahklun mountains, southwestern Alaska. Geology 30, 679–682.

Briner, J.P., Tulenko, J., Kaufman, D.S., Young, N.E., Baichtal, J., Lesnek, A., 2017. The last deglaciation of Alaska. Cuad. Invest. Geográfica. Geogr. Res. Lett. 43, 429–448.

Caissie, B.E., Brigham-Grette, J., Lawrence, K.T., Herbert, T.D., Cook, M.S., 2010. Last Glacial Maximum to Holocene sea surface conditions at Umnak Plateau, Bering Sea, as inferred from diatom, alkenone, and stable isotope records. Paleoceanography 25. https://doi.org/10.1029/2008PA001671.

Child, J., 1995. A Late Quaternary Lacustrine Record of Environmental Change in the Wonder Lake Area, Denali National Park and Preserve, Alaska. MS Thesis. University of Massachusetts at Amherst.

Clark, P.U., Shakun, J.D., Baker, P.A., Bartlein, P.J., Brewer, S., Brook, E., Carlson, A.E., Cheng, H., Kaufman, D.S., Liu, Z., 2012. Global climate evolution during the last deglaciation. Proc. Natl. Acad. Sci. Unit. States Am. 109, E1134–E1142.

COHMAP Members, 1988. Climatic changes of the last 18,000 years: observations and model simulations. Science 241, 1043–1052.

Corbett, L.B., Bierman, P.R., Rood, D.H., 2016. An approach for optimizing in situ cosmogenic ^{10}Be sample preparation. Quat. Geochronol. 33, 24–34.

Cosma, T., Hendy, I., 2008. Pleistocene glacimarine sedimentation on the continental slope off Vancouver Island, British Columbia. Mar. Geol. 255, 45–54.

Coulter, H., Hopkins, D., Karlstrom, T., Péwé, T., Wahrhaftig, C., Williams, J.R., 1965. Map showing extent of glaciations in Alaska: U.S. Geological Survey Miscellaneous Geologic Investigations Map, 415, p. 1 (sheet).

Dalton, A.S., Margold, M., Stokes, C.R., Tarasov, L., Dyke, A.S., Adams, R.S., Allard, S., Arends, H.E., Atkinson, N., Attig, J.W., Barnett, P.J., Barnett, R.L., Batterson, M., Bernatchez, P., Borns, H.W., Breckenridge, A., Briner, J.P., Brouard, E., Campbell, J.E., Carlson, A.E., Clague, J.J., Curry, B.B., Daigneault, R.-A., Dubé-Loubert, H., Easterbrook, D.J., Franzi, D.A., Friedrich, H.G., Funder, S., Gauthier, M.S., Gowan, A.S., Harris, K.L., Hétu, B., Hooyer, T.S., Jennings, C.E., Johnson, M.D., Kehew, A.E., Kelley, S.E., Kerr, D., King, E.L., Kjeldsen, K.K., Knaeble, A.R., Lajeunesse, P., Lakeman, T.R., Lamothe, M., Larson, P., Lavoie, M., Loope, H.M., Lowell, T.V., Lusardi, B.A., Manz, L., McMartin, I., Nixon, F.C., Occhietti, S., Parkhill, M.A., Piper, D.J.W., Pronk, A.G., Richard, P.J.H., Ridge, J.C., Ross, M., Roy, M., Seaman, A., Shaw, J., Stea, R.R., Teller, J.T., Thompson, W.B., Thorleifson, L.H., Utting, D.J., Veillette, J.J., Ward, B.C., Weddle, T.K., Wright, H.E., 2020. An updated radiocarbon-based ice margin chronology for the last deglaciation of the North American Ice Sheet Complex. Quat. Sci. Rev. 234, 106223. https://doi.org/10.1016/j.quascirev.2020.106223.

Daniels, W.C., Russell, J.M., Morrill, C., Longo, W.M., Giblin, A.E., Holland-Stergar, P., Welker, J.M., Wen, X., Hu, A., Huang, Y., 2021. Lacustrine leaf wax hydrogen isotopes indicate strong regional climate feedbacks in Beringia since the last ice age. Quat. Sci. Rev. 269, 107130. https://doi.org/10.1016/j.quascirev.2021.107130.

Dorfman, J., Stoner, J., Finkenbinder, M., Abbott, M., Xuan, C., St-Onge, G., 2015. A 37,000-year environmental magnetic record of aeolian dust deposition from Burial Lake, Arctic Alaska. Quat. Sci. Rev. 128, 81–97.

Dortch, J.M., Owen, L.A., Caffee, M.W., Brease, P., 2010a. Late Quaternary glaciation and equilibrium line altitude variations of the McKinley River region, central Alaska Range. Boreas 39, 233–246.

Dortch, J.M., Owen, L.A., Caffee, M.W., Li, D., Lowell, T.V., 2010b. Beryllium-10 surface exposure dating of glacial successions in the Central Alaska Range. J. Quat. Sci. 25, 1259–1269.
Duk-Rodkin, A., 1999. Glacial Limits Map of Yukon. Indian & Northern Affairs Canada/Department of Indian & Northern Development: Exploration & Geological Services Division. Geoscience Mapp. 1999–2.
Elias, S.A., Short, S.K., Nelson, C.H., Birks, H.H., 1996. Life and times of the Bering land bridge. Nature 382, 60–63.
England, J.H., Furze, M.F., 2008. New evidence from the western Canadian Arctic Archipelago for the resubmergence of Bering Strait. Quat. Res. 70, 60–67.
Finkenbinder, M., Abbott, M., Finney, B., Stoner, J., Dorfman, J., 2015. A multi-proxy reconstruction of environmental change spanning the last 37,000 years from Burial Lake, Arctic Alaska. Quat. Sci. Rev. 126, 227–241.
Finkenbinder, M.S., Abbott, M.B., Edwards, M.E., Langdon, C.T., Steinman, B.A., Finney, B.P., 2014. A 31,000 year record of paleoenvironmental and lake-level change from Harding Lake, Alaska, USA. Quat. Sci. Rev. 87, 98–113.
Haeussler, P.J., Matmon, A., Arnold, M., Aumaître, G., Bourlès, D., Keddadouche, K., 2021. Late quaternary deglaciation of Prince William Sound, Alaska. Quat. Res. 105, 1–20.
Hall, B.L., Denton, G., Lowell, T., Bromley, G., Putnam, A., 2017. Retreat of the Cordillera Darwin icefield during the termination I. Cuad. Invest. Geográfica. Geogr. Res. Lett. 43, 751–766.
Hamilton, T.D., 1994. Late Cenozoic glaciation of Alaska. In: Plafker, G., Berg, H.C. (Eds.), The Geology of Alaska. Geological Society of America. https://doi.org/10.1130/DNAG-GNA-G1.813.
Hamilton, T.D., 1986. Late Cenozoic glaciation of the central Brooks range. In: Hamilton, T.D., et al. (Eds.), Glaciation in Alaska: the Geologic Record: Anchorage. Alaska Geological Society, pp. 9–50.
Hamilton, T.D., Reed, K.M., Thorsen, R., 1986. Glaciation in Alaska: the Geologic Record: Anchorage. Alaska Geological Society.
Harrison, A., 1964. Ice surges on the Muldrow Glacier, Alaska. J. Glaciol. 5, 365–368.
Howley, M.W., 2008. A Late Glacial and Holocene Chronology of the Castner Glacier, Delta River Valley, Alaska. MS Thesis. University of New Hampshire.
Ibarra, D.E., Egger, A.E., Weaver, K.L., Harris, C.R., Maher, K., 2014. Rise and fall of late Pleistocene pluvial lakes in response to reduced evaporation and precipitation: evidence from Lake Surprise, California. Geol. Soc. Am. Bull. 126, 1387–1415.
Jakobsson, M., Pearce, C., Cronin, T.M., Backman, J., Anderson, L.G., Barrientos, N., Björk, G., Coxall, H., De Boer, A., Mayer, L.A., 2017. Post-glacial flooding of the Bering Land Bridge dated to 11 cal ka BP based on new geophysical and sediment records. Clim. Past 13, 991–1005.
Kaufman, D.S., Anderson, R.S., Hu, F.S., Berg, E., Werner, A., 2010. Evidence for a variable and wet Younger Dryas in southern Alaska. Quat. Sci. Rev. 29, 1445–1452.
Kaufman, D.S., Hu, F.S., Briner, J.P., Werner, A., Finney, B.P., Gregory-Eaves, I., 2003. Ã 33,000 year record of environmental change from Arolik lake, Ahklun mountains, Alaska, USA. J. Paleolimnol. 30, 343–361.
Kaufman, D.S., Jensen, B.J., Reyes, A.V., Schiff, C.J., Froese, D.G., Pearce, N.J., 2012. Late quaternary tephrostratigraphy, Ahklun mountains, SW Alaska. J. Quat. Sci. 27, 344–359.
Kaufman, D.S., Manley, W.F., 2004. Pleistocene Maximum and Late Wisconsinan glacier extents across Alaska, U.S.A. In: Ehlers, J., Gibbard, P.L. (Eds.), Developments in Quaternary Sciences. Elsevier, pp. 9–27. https://doi.org/10.1016/S1571-0866(04)80182-9.
Kaufman, D.S., Young, N.E., Briner, J.P., Manley, W.F., 2011. Alaska Palaeo-Glacier Atlas (Version 2). In: Ehlers, J., Gibbard, P.L., Hughes, P.D. (Eds.), Developments in Quaternary Sciences. Elsevier, pp. 427–445. https://doi.org/10.1016/B978-0-444-53447-7.00033-7.
Kline, J.T., Bundtzen, T.K., 1986. Two glacial records from west-central Alaska. Alaska Geological Society, Anchorage. Alaska, Glaciation in Alaska. In: Hamilton, T.D., et al. (Eds.), Glaciation in Alaska: the Geologic Record: Anchorage. Alaska Geological Society, pp. 123–150.
Kohl, C., Nishiizumi, K., 1992. Chemical isolation of quartz for measurement of in-situ-produced cosmogenic nuclides. Geochem. Cosmochim. Acta 56, 3583–3587.
Kopczynski, S.E., Kelley, S.E., Lowell, T.V., Evenson, E.B., Applegate, P.J., 2017. Latest Pleistocene advance and collapse of the Matanuska–Knik glacier system, Anchorage Lowland, southern Alaska. Quat. Sci. Rev. 156, 121–134.
Kurek, J., Cwynar, L.C., Ager, T.A., Abbott, M.B., Edwards, M.E., 2009. Late Quaternary paleoclimate of western Alaska inferred from fossil chironomids and its relation to vegetation histories. Quat. Sci. Rev. 28, 799–811.
Laabs, B.J.C., Licciardi, J.M., Leonard, E.M., Munroe, J.S., Marchetti, D.W., 2020. Updated cosmogenic chronologies of Pleistocene mountain glaciation in the western United States and associated paleoclimate inferences. Quat. Sci. Rev. 242, 106427. https://doi.org/10.1016/j.quascirev.2020.106427.
Lal, D., 1991. Cosmic ray labeling of erosion surfaces: in situ nuclide production rates and erosion models. Earth Planet Sci. Lett. 104, 424–439.
Lanphere, M.A., Reed, B.L., 1985. The McKinley sequence of granitic rocks: A key element in the accretionary history of southern Alaska. J. Geophys. Res. Solid Earth 90, 11413–11430.
Laskar, J., Robutel, P., Joutel, F., Gastineau, M., Correia, A.C.M., Levrard, B., 2004. A long-term numerical solution for the insolation quantities of the Earth. Astron. Astrophys. 428, 261–285. https://doi.org/10.1051/0004-6361:20041335.
Lesnek, A.J., Briner, J.P., Baichtal, J.F., Lyles, A.S., 2020. New constraints on the last deglaciation of the Cordilleran Ice Sheet in coastal Southeast Alaska. Quat. Res. 96, 140–160.
Lesnek, A.J., Briner, J.P., Lindqvist, C., Baichtal, J.F., Heaton, T.H., 2018. Deglaciation of the Pacific coastal corridor directly preceded the human colonization of the Americas. Sci. Adv. 4, 5040.
Levy, L.B., Kaufman, D.S., Werner, A., 2004. Holocene glacier fluctuations, Waskey Lake, northeastern Ahklun Mountains, southwestern Alaska. Holocene 14, 185–193.
Liakka, J., Lofverstrom, M., 2018. Arctic warming induced by the Laurentide Ice Sheet topography. Clim. Past 14, 887–900. https://doi.org/10.5194/cp-14-887-2018.
Löfverström, M., Liakka, J., 2016. On the limited ice intrusion in Alaska at the LGM. Geophys. Res. Lett. 43, 11. https://doi.org/10.1002/2016GL071012, 030-11,038.
Löfverström, M., Lora, J.M., 2017. Abrupt regime shifts in the North Atlantic atmospheric circulation over the last deglaciation. Geophys. Res. Lett. 44, 8047–8055.
Lora, J.M., Ibarra, D.E., 2019. The North American hydrologic cycle through the last deglaciation. Quat. Sci. Rev. 226, 105991. https://doi.org/10.1016/j.quascirev.2019.105991.
Lora, J.M., Mitchell, J.L., Tripati, A.E., 2016. Abrupt reorganization of North Pacific and western North American climate during the last deglaciation. Geophys. Res. Lett. 43 (11), 796. https://doi.org/10.1002/2016GL071244, 11,804.
Manley, W.F., Kaufman, D.S., Briner, J.P., 2001. Pleistocene glacial history of the southern Ahklun Mountains, southwestern Alaska: Soil-development, morphometric, and radiocarbon constraints. Quat. Sci. Rev. 20, 353–370.
Mann, D.H., Peteet, D.M., 1994. Extent and timing of the last glacial maximum in southwestern Alaska. Quat. Res. 42, 136–148.
Matmon, A., Briner, J., Carver, G., Bierman, P., Finkel, R., 2010. Moraine chronosequence of the Donnelly Dome region, Alaska. Quat. Res. 74, 63–72.
Moreno, P.I., Denton, G.H., Moreno, H., Lowell, T.V., Putnam, A.E., Kaplan, M.R., 2015. Radiocarbon chronology of the last glacial maximum and its termination in northwestern Patagonia. Quat. Sci. Rev. 122, 233–249.
NGRIP members, 2004. High resolution record of Northern Hemisphere climate extending into the last interglacial period. Nature 431, 147–151.
Oerlemans, J., 2005. Extracting a climate signal from 169 glacier records. Science 308, 675–677. https://doi.org/10.1126/science.1107046.
Osman, M.B., Tierney, J.E., Zhu, J., Tardif, R., Hakim, G.J., King, J., Poulsen, C.J., 2021. Globally resolved surface temperatures since the Last Glacial Maximum. Nature 599, 239–244.
Otto-Bliesner, B.L., Brady, E.C., Clauzet, G., Tomas, R., Levis, S., Kothavala, Z., 2006. Last Glacial Maximum and Holocene Climate in CCSM3. J. Clim. 19, 2526–2544. https://doi.org/10.1175/JCLI3748.1.
Palacios, D., Stokes, C.R., Phillips, F.M., Clague, J.J., Alcalá-Reygosa, J., Andrés, N., Angel, I., Blard, P.-H., Briner, J.P., Hall, B.L., 2020. The deglaciation of the Americas during the Last Glacial Termination. Earth Sci. Rev. 203, 103113.
Pedro, J., Van Ommen, T., Rasmussen, S., Morgan, V., Chappellaz, J., Moy, A., Masson-Delmotte, V., Delmotte, M., 2011. The last deglaciation: timing the bipolar seesaw. Clim. Past 7, 671–683.
Pedro, J.B., Bostock, H.C., Bitz, C.M., He, F., Vandergoes, M.J., Steig, E.J., Chase, B.M., Krause, C.E., Rasmussen, S.O., Markle, B.R., 2016. The spatial extent and dynamics of the Antarctic Cold Reversal. Nat. Geosci. 9, 51–55.
Peltier, C., Kaplan, M.R., Birkel, S.D., Soteres, R.L., Sagredo, E.A., Aravena, J.C., Araos, J., Moreno, P.I., Schwartz, R., Schaefer, J.M., 2021. The large MIS 4 and long MIS 2 glacier maxima on the southern tip of South America. Quat. Sci. Rev. 262, 106858.
Peltier, W.R., Argus, D.F., Drummond, R., 2015. Space geodesy constrains ice age terminal deglaciation: The global ICE-6G_C (VM5a) model. J. Geophys. Res. Solid Earth 120, 450–487. https://doi.org/10.1002/2014JB011176.
Pendleton, S.L., Ceperley, E.G., Briner, J.P., Kaufman, D.S., Zimmerman, S., 2015. Rapid and early deglaciation in the central Brooks Range, Arctic Alaska. Geology 43, 419–422. https://doi.org/10.1130/G36430.1.
Porter, S.C., Pierce, K.L., Hamilton, T.D., 1983. Late Wisconsin mountain glaciation in the western United States. In Late Quaternary Environments of the United States. In: Porter, S.C. (Ed.), The Late Pleistocene, vol. 1. University of Minnesota Press, Minneapolis, pp. 71–111.
Praetorius, S.K., Condron, A., Mix, A.C., Walczak, M.H., McKay, J.L., Du, J., 2020. The role of Northeast Pacific meltwater events in deglacial climate change. Sci. Adv. 6, eaay2915. https://doi.org/10.1126/sciadv.aay2915.
Putnam, A.E., Denton, G.H., Schaefer, J.M., Barrell, D.J., Andersen, B.G., Finkel, R.C., Schwartz, R., Doughty, A.M., Kaplan, M.R., Schlüchter, C., 2010. Glacier advance in southern middle-latitudes during the Antarctic Cold Reversal. Nat. Geosci. 3, 700–704.
Putnam, A.E., Schaefer, J.M., Denton, G.H., Barrell, D.J., Birkel, S.D., Andersen, B.G., Kaplan, M.R., Finkel, R.C., Schwartz, R., Doughty, A.M., 2013. The last glacial maximum at 44 S documented by a ^{10}Be moraine chronology at Lake Ohau, Southern Alps of New Zealand. Quat. Sci. Rev. 62, 114–141.
Rasmussen, S.O., Bigler, M., Blockley, S.P., Blunier, T., Buchardt, S.L., Clausen, H.B., Cvijanovic, I., Dahl-Jensen, D., Johnsen, S.J., Fischer, H., 2014. A stratigraphic framework for abrupt climatic changes during the Last Glacial period based on three synchronized Greenland ice-core records: refining and extending the INTIMATE event stratigraphy. Quat. Sci. Rev. 106, 14–28.
Reger, R.D., Sturmann, A.G., Berg, E.E., Burns, P.A.C., 2007. A Guide to the Late Quaternary History of Northern and Western Kenai Peninsula, vol. 8. Alaska Division of Geological & Geophysical Surveys Guidebook, Alaska, p. 112. https://doi.org/10.14509/15941, 6 sheets, scale 1:63,360.
Reheis, M.C., Adams, K.D., Oviatt, C.G., Bacon, S.N., 2014. Pluvial lakes in the Great Basin of the western United States—a view from the outcrop. Quat. Sci. Rev. 97,

33–57. https://doi.org/10.1016/j.quascirev.2014.04.012.
Roe, G.H., Baker, M.B., Herla, F., 2017. Centennial glacier retreat as categorical evidence of regional climate change. Nat. Geosci. 10, 95–99. https://doi.org/10.1038/ngeo2863.
Roe, G.H., Lindzen, R.S., 2001. The mutual interaction between continental-scale ice sheets and atmospheric stationary waves. J. Clim. 14, 1450–1465. https://doi.org/10.1175/1520-0442(2001)014<1450:TMIBCS>2.0.CO;2.
Seltzer, A.M., Ng, J., Aeschbach, W., Kipfer, R., Kulongoski, J.T., Severinghaus, J.P., Stute, M., 2021. Widespread six degrees Celsius cooling on land during the Last Glacial Maximum. Nature 593, 228–232.
Shakun, J.D., Clark, P.U., He, F., Lifton, N.A., Liu, Z., Otto-Bliesner, B.L., 2015. Regional and global forcing of glacier retreat during the last deglaciation. Nat. Commun. 6, 1–7.
Shakun, J.D., Clark, P.U., He, F., Marcott, S.A., Mix, A.C., Liu, Z., Otto-Bliesner, B., Schmittner, A., Bard, E., 2012. Global warming preceded by increasing carbon dioxide concentrations during the last deglaciation. Nature 484, 49–54.
Sheinkman, V.S., 2011. Glaciation in the High Mountains of Siberia. In: Ehlers, J., Gibbard, P.L., Hughes, P.D. (Eds.), Developments in Quaternary Sciences. Elsevier, pp. 883–907. https://doi.org/10.1016/B978-0-444-53447-7.00065-9.
Stone, J.O., 2000. Air pressure and cosmogenic isotope production. J. Geophys. Res. Solid Earth 105, 23753–23759.
Ten Brink, N.W., Waythomas, C.F., 1985. Late Wisconsin glacial chronology of the north-central Alaska Range: a regional synthesis and its implications for early human settlements. In: Powers, W.R., et al. (Eds.), North Alaska Range Early Man Project. National Geographic Society Research Reports, National. Geographic Society, Washington, DC, pp. 15–32.
Tierney, J.E., Zhu, J., King, J., Malevich, S.B., Hakim, G.J., Poulsen, C.J., 2020. Glacial cooling and climate sensitivity revisited. Nature 584, 569–573.
Tulenko, J.P., Briner, J.P., Young, N.E., Schaefer, J.M., 2018. Beryllium-10 chronology of early and late Wisconsinan moraines in the Revelation Mountains, Alaska: Insights into the forcing of Wisconsinan glaciation in Beringia. Quat. Sci. Rev. 197, 129–141. https://doi.org/10.1016/j.quascirev.2018.08.009.
Tulenko, J.P., Caffee, W., Schweinsberg, A.D., Briner, J.P., Leonard, E.M., 2020a. Delayed and rapid deglaciation of alpine valleys in the Sawatch Range, southern Rocky Mountains, USA. Geochronology 2, 245–255.
Tulenko, J.P., Lofverstrom, M., Briner, J.P., 2020b. Ice sheet influence on atmospheric circulation explains the patterns of Pleistocene alpine glacier records in North America. Earth Planet Sci. Lett. 534, 116115.
Valentino, J.D., Owen, L.A., Spotila, J.A., Cesta, J.M., Caffee, M.W., 2021. Timing and extent of Late Pleistocene glaciation in the Chugach Mountains, Alaska. Quat. Res. 101, 205–224.
Viau, A., Gajewski, K., Sawada, M., Bunbury, J., 2008. Low-and high-frequency climate variability in eastern Beringia during the past 25 000 years. Can. J. Earth Sci. 45, 1435–1453.
Wang, Y.-J., Cheng, H., Edwards, R.L., An, Z., Wu, J., Shen, C.-C., Dorale, J.A., 2001. A high-resolution absolute-dated late Pleistocene monsoon record from Hulu Cave, China. Science 294, 2345–2348.
Werner, A., Wright, K., Child, J., 1993. Bluff Stratigraphy along the McKinley River: a Record of Late Wisconsin Climatic Change, vol. 25. Geological Society of America Abstracts with Programs, p. 224.
Whitmore, J., Gajewski, K., Sawada, M., Williams, J.W., Shuman, B., Bartlein, P.J., Minckley, T., Viau, A.E., Webb, T., Shafer, S., Anderson, P., Brubaker, L., 2005. Modern pollen data from North America and Greenland for multi-scale paleoenvironmental applications. Quat. Sci. Rev. 24, 1828–1848. https://doi.org/10.1016/j.quascirev.2005.03.005.
Young, N.E., Briner, J.P., Kaufman, D.S., 2009. Late Pleistocene and Holocene glaciation of the Fish Lake valley, northeastern Alaska Range, Alaska. J. Quat. Sci. 24, 677–689.
Young, N.E., Briner, J.P., Leonard, E.M., Licciardi, J.M., Lee, K., 2011. Assessing climatic and nonclimatic forcing of Pinedale glaciation and deglaciation in the western United States. Geology 39, 171–174.
Young, N.E., Briner, J.P., Schaefer, J., Zimmerman, S., Finkel, R.C., 2019. Early Younger Dryas glacier culmination in southern Alaska: Implications for North Atlantic climate change during the last deglaciation. Geology 47, 550–554.
Young, N.E., Schaefer, J.M., Briner, J.P., Goehring, B.M., 2013. A 10 B e production-rate calibration for the Arctic. J. Quat. Sci. 28, 515–526.